Dr. Trevor Keenan   April 29ᵗʰ, 2015
Associate Editor, Biogeosciences

Dear Dr. Keenan,

We are very pleased with the positive evaluation of our revised paper bg-2014-567 (Assessing vegetation structure and ANPP dynamics in a grassland-shrubland Chihuahuan ecotone using NDVI-rainfall relationships).

Please, find below a complete list of answers to the comments raised by Reviewer#1 and yourself for publication of our manuscript.

Looking forward to hearing from you soon.

On behalf of the co-authors,
Kind regards,

Mariano Moreno de las Heras

Dr. Mariano Moreno de las Heras
Marie Curie Research Fellow
Department of Geography
Durham University, UK
Phone: +44 (0) 191 33 41829
Fax: +44 (0) 191 33 41801
mariano.moreno-de-las-heras@durham.ac.uk
https://www.dur.ac.uk/geography/staff/geogstaffhidden/?id=11733

1. Comments by Dr. Trevor Keenan (Associate Editor):

Let me start by apologizing for the length of time it has taken to handle your manuscript for Biogeosciences. I am pleased to let you know that the reviewers have assessed your reply to their initial comments and find your manuscript much improved. They suggest publication, but Reviewer 1 has a few suggestions where your manuscript could be further improved. I would appreciate it if you could seriously consider these suggestions, but also find that significantly reworking the statistical analysis at this stage is unnecessary.

Reply to Trevor Keenan's comments:
We are very pleased with the positive evaluation of the changes in our revised manuscript and your decision to publish the paper subject to technical corrections.

We have thoughtfully considered Reviewer#1 comments and suggestions for improving the paper. Briefly, Reviewer#1's comments underscore his/her preferences for an alternative study approach, based on direct application of a modelling framework for the objectives of our study. As explained in our previous revision, we think that the suggested approach is not feasible and that our semi-empirical study approach provides the best analytical framework for the objectives of our paper. Please, note that application of the suggested approach would imply re-working entirely the study, generating a totally different work. In this response

letter, we have done our best to clarify the issues indicated by Referee#1, applying minimal modifications in our paper.

2. Comments by Referee#1:

Comment 2.1: *The authors have provided a detailed list of answers to my comments on the first version of this manuscript. I appreciate their efforts to better explain their point of view although I am not entirely convinced by some of their choice (see below). I acknowledge that a number of clarifications have been made and that the manuscript has improved because of these changes.*

Reply to Comment 2.1:
We very appreciate the positive evaluation of our responses and modifications included in the revised paper.

Comment 2.2: *There has been a misunderstanding of my comments regarding model structure. I did not call for a more complex model than the one presented in the first section, as it is obvious that the available empirical data would not allow to properly calibrating and validating it. I fully reckon the merit of low-dimensional model that capture the essentials of ecohydrological dynamics in drylands and that could be easily confronted to time series of vegetation greenness. The limitations of these models should be discussed and, above all, their overall performance to represent ecosystem functioning and dynamics should be assessed. The authors have provided evidence to meet these requirements. In the context of this study, I understand the usefulness of introducing a simple and process-oriented model of the coupled dynamics between plant growth and soil water availability. I still regret that the presentation of this model is somewhat disconnected from the remote sensing study. Once again, I would have preferred a phenomenological analysis of greenness with a statistical approch emphasizing the effect of precedent cumulative rainfall on plant growth. This should conduct to optimize the parameters Olrs and Olrh and to provide the rationale for a NDVI decomposition in mixed stands. In a further step, it could be shown that the parameter estimates (57 and 145 days) are consistent with the Rietkerk conceptual model providing certain combination of plant growth and plant mortality rates (isolines of figure 1 c) and given a fixed set of values for the other parameters. Then it should be mentionned that published parameters (gmax and m) for grass and shrubs fall in the range of inferred values using optimized Olr but also that NDVI data alone do not provide enough constraint to narrow the domain of plausible values. I have the feeling that this would provide a tighter connection between the two sections of the manuscript. In this logic, the first estimates of optimal rainfall accumulation length (Olr) using parameters from the litterature are unnecessary.*

Reply to Comment 2.2:
The purpose of the application of the simple model introduced in our study is to offer a conceptual biophysical explanation of the time-scale dependencies of plant biomass-rainfall

responses on vegetation type that are extensively studied in our paper (Page 4, lines 25-28). The model constitutes a fully comprehensive conceptual framework for the empirical relationships determined and applied in our remote-sensing analysis. For example, the presentation of the model facilitates the introduction and clear description, in the initial part of the paper, of the empirical NDVI-rainfall metrics (i.e. *Olr* values and *ARain* antecedent rainfall series) that were obtained and further applied in the remote-sensing analysis of our study (Pages 6-7, lines 20-14). In addition, the model provides a biophysical explanation for the contrasting *Olr* values and *ARain* series empirically determined for the different vegetation types in the studied ecotone as a function of their characteristic patterns of plant growth and water use (with herbaceous vegetation showing quick phenological responses to short-term rainfall and shrubs showing slow responses to longer-term antecedent precipitation; Page 19, lines 1-28). The model is therefore fully connected with the remote-sensing analysis of our study.

Referee#1 suggests that direct application of the simple process-based model presented in the paper for optimizing the *Olr* metrics and modelling the time series of NDVI could provide a tighter connection between the different parts of the paper than our semi-empirical study approach. Our model provides a good starting point for addressing, from a conceptual point of view, differences in plant responses to antecedent precipitation for herbaceous and shrub vegetation in drylands. Furthermore, it does provide a robust, statistical basis for the estimation of the empirical metrics/parameters required by our remote-sensing analysis without the need for further optimization. However, we believe that direct application of a fully process-based modelling approach for decomposing/estimating ground-based NPP for different types of vegetation in mixed systems would necessarily require a more complex framework than the simple model presented in our study. For example, the equations of the model should at least combine the biomass dynamics of the different vegetation types, including plant-plant interactions between the herbaceous and shrub components of vegetation for mixed systems (note that in the simple model included in our paper the dynamics of the different vegetation types can be analyzed separately, but does not describe combined dynamics in mixed systems). The use of semi-empirical study approaches, as the one developed in our paper, facilitates optimization of results with a low degree of complexity. Our study approach applies empirically determined vegetation-type specific NDVI-rainfall metrics (characteristic *Olr* values and *ARain* series for herbaceous and shrub vegetation) as lumped (or black-box) spatiotemporal criteria to classify landscape types and decompose NDVI time series into herbaceous and shrub components of landscape ANPP. The study approach proved to accurately determine the spatial structure of vegetation types and spatiotemporal ANPP dynamics at the studied grassland-shrubland ecotone. In addition, we think that the different parts of the study are well integrated throughout the paper and facilitate easy understanding of the methods and results by the readers. Overall, we believe that our semi-empirical study approach provides the best analytical framework for the objectives of our paper.

Comment 2.3: *I am not very satisfied with the answer to my comments on the performance of the NDVI decomposition. Obviously, we are talking about the assessment of model*

performance when considering the entire time series (not a single ti). Consider a MODIS pixel with known percentages of shrub and grass cover, reconstruct the time series of greenness/biomass for this mixed stand using the observed rainfalls and the optimized parameters Olrh and Olrs, how much of the observed NDVI dynamics are you capturing? how does the bivariate relationship between modelled and predicted NDVI looks like?

Reply to Comment 2.3:

The purpose of the NDVI decomposition method we applied in our study is neither modelling the NDVI dynamics nor estimating vegetation cover, but partitioning the NDVI temporal series into components of herbaceous and shrub vegetation for the estimation of ANPP. We provide a detailed analysis of the performance of the NDVI decomposition and transformation procedure in our study. The partitioned NDVI components of herbaceous and shrub vegetation explain about 66% data variability on ground-based ANPP, resulting in a very low degree of normalized root mean square error (about 10%) for our remote-sensing estimations of herbaceous and shrub ANPP. As detailed in the paper (Pages 20-21, lines 31-11), this constitutes a great achievement for arid and semiarid landscapes, where field ANPP is very importantly affected by data dispersion due to vegetation patchiness. Since the objective of the NDVI decomposition method in our work is the estimation of NPP temporal series, evaluation of the method against temporal series of vegetation cover (which are unavailable for our site) or back-to-front analysis of the ANPP temporal series against the NDVI dynamics has not particular interest for the study.

As any other NDVI decomposition methods published in literature, our approach does not alter in any way the original NDVI values in the partition. In other words, the computed soil background baseline value (0.12) plus the partitioned NDVI levels for herbaceous vegetation (C_{hv}) and the shrub component (C_s) totals the NDVI values of the original temporal series. To clarify this point, we have added the following information in the methods: Page 13, lines 19-20: "Computed soil background baseline, C_{bs}, plus the partitioned NDVI components for herbaceous vegetation, C_{hv}, and shrubs, C_s, total the original NDVI levels of the temporal series for any point in time and space".

Assessing vegetation structure and ANPP dynamics in a grassland-shrubland Chihuahuan ecotone using NDVI-rainfall relationships

M. Moreno-de las Heras[1], R. Díaz-Sierra[2], L. Turnbull[1], J. Wainwright[1]

[1]{Department of Geography, Durham University, Durham DH1 3LE, United Kingdom}

[2]{Mathematical and Fluid Physics Department, Faculty of Sciences, UNED, Madrid 28040, Spain}

Correspondence to: M. Moreno-de las Heras (mariano.moreno-de-las-heras@durham.ac.uk)

Abstract

Climate change and the widespread alteration of natural habitats are major drivers of vegetation change in drylands. In the Chihuahuan Desert, large areas of grasslands dominated by perennial grass species have transitioned over the last 150 years to shrublands dominated by woody species, accompanied by accelerated water and wind erosion. Multiple mechanisms drive the shrub-encroachment process, including precipitation variations, land-use change, and soil erosion-vegetation feedbacks. In this study, using a simple ecohydrological modelling framework, we show that herbaceous (grasses and forbs) and shrub vegetation in drylands have different responses to antecedent precipitation due to functional differences in plant growth and water-use patterns. Therefore, shrub encroachment may be reflected in the analysis of landscape-scale vegetation-rainfall relationships. We analyze the structure and dynamics of vegetation at an 18 km^2 grassland-shrubland ecotone in the northern edge of the Chihuahuan Desert (McKenzie Flats, Sevilleta National Wildlife Refuge, NM, USA) by investigating the relationship between decade-scale (2000-13) records of remotely sensed vegetation greenness (MODIS NDVI) and antecedent rainfall. NDVI-rainfall relationships show a high sensitivity to spatial variations on dominant vegetation types across the grassland-shrubland ecotone, and provide ready biophysical criteria to (a) classify landscape types as a function of the spatial distribution of dominant vegetation, and to (b) decompose the NDVI signal into partial components of annual net primary production (ANPP) for

1 herbaceous vegetation and shrubs. Analysis of remote-sensed ANPP dynamics across the
2 study site indicates that plant growth for herbaceous vegetation is particularly synchronized
3 with monsoonal summer rainfall. For shrubs, ANPP is better explained by winter plus
4 summer precipitation, overlapping the monsoonal period (June to September) of rain
5 concentration. Our results suggest that shrub encroachment has not been particularly active in
6 this Chihuahuan ecotone for 2000-13. However, future changes in the amount and temporal
7 pattern of precipitation (i.e. reductions in monsoonal summer rainfall and/or increases in
8 winter precipitation) may enhance the shrub-encroachment process, particularly in the face of
9 expected upcoming increases in aridity for desert grasslands of the American Southwest.

10

11 1   Introduction

12 Land degradation is pervasive across many dryland regions, which cover over 40% of the
13 Earth's surface and account for about 30% of global terrestrial net primary productivity,
14 globally supporting about 2.5 billion inhabitants (Millennium Ecosystem Assessment, 2005).
15 Over recent decades these dryland regions have experienced growing human and climatic
16 pressures. The most dramatic landscape alterations resulting from these pressures are those
17 associated with desertification, which are perceived as catastrophic and largely irreversible
18 changes that can ultimately lead to relatively barren ecosystem states (Schlesinger et al.,
19 1990; Okin et al., 2009). A common form of vegetation change in drylands involves the
20 encroachment of desert shrub species into arid and semi-arid grasslands, which has already
21 affected more than 250 million hectares worldwide throughout the US, South America,
22 Southern Africa and Australia (D'Odorico et al., 2012; Turnbull et al., 2014).

23 A classic case of vegetation shift is the shrub-encroachment process that has been taking place
24 over the last 150 years in the Chihuahuan Desert in south-western USA and northern Mexico,
25 where large areas of grasslands dominated by C_4 perennial grass species (black grama,
26 *Bouteloua eriopoda*, and blue grama, *B. gracilis*) have been replaced by shrublands
27 dominated by C_3 desert shrub species (mainly creosotebush, *Larrea tridentata*, and honey
28 mesquite, *Prosopis glandulosa*). These changes in vegetation have been accompanied by
29 accelerated water and wind erosion (for example, Schlesinger et al., 1990; Wainwright et al.,
30 2000; Mueller et al., 2007; Turnbull et al., 2010a; Ravi et al., 2010). A complex range of
31 mechanisms have been suggested to explain the occurrence of this vegetation transition,
32 including external drivers that initiate the transition, and endogenous soil erosion-vegetation

2

feedbacks that further drive vegetation change (Turnbull et al., 2012). These internal feedbacks strongly alter the organization and distribution of both vegetation and soil resources (i.e. substrate, soil moisture and nutrients), strengthening the vegetation-change process (Okin et al., 2009; Turnbull et al., 2010b, 2012; Stewart et al., 2014).

The onset of the grassland-shrubland transition in the Chihuahuan Desert is thought to have started with the introduction of large numbers of domestic grazers, which may have favored the establishment of pioneer shrubs via the creation of gaps (Buffington and Herbel, 1965; van Auken, 2000; Webb et al., 2003) and via a reduction in the frequency and intensity of natural wildfires (D'Odorico et al., 2012). Changing rainfall amount and frequency has also been invoked as one of the major external drivers of shrub encroachment, which may contribute to vegetation change by shifting competitive plant physiological advantages of grass and desert shrub species (Gao and Reynolds, 2003; Snyder and Tartowsky, 2006; Throop et al., 2012). However, there remains a lack of consensus regarding changes in rainfall in the southwest USA over recent decades. Whilst Petrie et al. (2014) found no significant changes in precipitation at the Sevilleta Long Term Ecological Research Site in central New Mexico, other studies have reported significant increases in both annual and winter precipitation at the Jornada Experimental Range in southern New Mexico, but concurrent decreases in the size of discrete precipitation events (Wainwright, 2006; Turnbull et al., 2013).

Comprehensive understanding of how desert grasslands are responding to the present variability on both climate and land use is critical for environmental management, especially in consideration of uncertainty regarding future climate change across many dryland regions. Remote sensing of vegetation provides a valuable source of information for landscape monitoring and forecasting of vegetation change in drylands (Okin and Roberts, 2004; Pennington and Collins, 2007; Moreno-de las Heras et al., 2012). Satellite-derived chlorophyll-sensitive vegetation indices, such as the Normalized Difference Vegetation Index (NDVI), provide important information on vegetation structure (e.g. surface cover, aboveground green biomass, vegetation type) and dynamics over broad spatial domains (Anderson et al., 1993; Peters et al., 1997; Weiss et al., 2004; Pettorelli et al., 2005; Choler et al., 2010; Forzieri et al., 2011).

In drylands, where vegetation dynamics are particularly well coupled with rainfall patterns, the relationship between time series of NDVI and precipitation provides specific information

1   on the use of water for the production and maintenance of plant biomass (Pennington and

2   Collins, 2007; Notaro et al., 2010; Veron and Paruelo, 2010). Investigations of the

3   relationships between NDVI and rainfall suggest that arid and semi-arid vegetation responds

4   to antecedent (or preceding cumulative) precipitation rather than to immediate rainfall, since

5   plant growth is affected by the history of available soil moisture (Al-Bakri and Suleiman,

6   2004; Schwinning and Sala, 2004; Evans and Geerken, 2004; Moreno-de las Heras et al.,

7   2012). The length (or number of days) of antecedent rainfall that best explains the NDVI (or

8   green biomass) dynamics of dryland vegetation (hereafter optimal length of rainfall

9   accumulation, *Olr*) appears to be site-specific and strongly dependent on vegetation type

10   (Evans and Geerken, 2004; Prasad et al., 2007; Garcia et al., 2010). Herbaceous vegetation

11   (i.e. grass and forb life-forms) and shrubs usually show important differences in the patterns

12   of vegetation growth and water-use, which mediate the responses of plant biomass to rainfall

13   in drylands (Ogle and Reynolds, 2004; Gilad et al., 2007; Pennington and Collins, 2007;

14   Forzieri et al., 2011; Stewart et al., 2014). Thus, the study of the relationship between the

15   NDVI and rainfall may offer important clues for detecting broad-scale landscape changes

16   involving grassland-shrubland transitions in arid and semi-arid landscapes.

17   The aim of this study is to analyze vegetation structure and dynamics at a Chihuahuan

18   grassland-shrubland ecotone (McKenzie Flats, Sevilleta National Wildlife Refuge, New

19   Mexico, USA). To fulfil this aim we explore the relationship between decade-scale (2000-13)

20   records of remote-sensed vegetation greenness (MODIS NDVI) and rainfall. Our analysis is

21   based on a new approach that examines characteristic NDVI-rainfall relationships for

22   dominant vegetation types (i.e. herbaceous vegetation and woody shrubs) to investigate the

23   organization and dynamics of vegetation as a way of evaluating how the shrub-encroachment

24   process occurs.

25   This paper is organized in two parts. First, we present the conceptual underpinning and

26   theoretical basis of our study, by using a simple, process-based ecohydrological model to

27   illustrate the biophysical control of the relationship between plant biomass dynamics and

28   antecedent rainfall for dryland herbaceous and shrub vegetation. Secondly, we empirically

29   determine reference optimal lengths of rainfall accumulation (in days) for herbaceous and

30   shrub vegetation (Olr_{hv} and Olr_s) in a 18 km^2 Chihuahuan ecotone, and use these vegetation-

31   type specific NDVI-rainfall metrics to (i) analyze the spatial organization and dynamics of net

32   primary production (NPP) for herbaceous vegetation and shrubs, and to (ii) explore the impact

1   of inter-annual variations in seasonal rainfall on the dynamics of vegetation production at the

2   grassland-shrubland ecotone.

3

4   2   Theoretical basis: herbaceous and shrub plant biomass-rainfall
5   relationships in drylands

6   Dryland herbaceous vegetation (i.e. grass and forb life-forms) and shrubs usually exhibit

7   important differences in the patterns of vegetation growth and water-use. Herbaceous

8   vegetation typically shows quick and intense growth pulses synchronized with major rainfall

9   events, while the dynamics of plant biomass for shrubs is generally less variable in time

10   (Sparrow et al., 1997; Lu et al., 2003; Garcia et al., 2010). These dissimilar growth responses

11   are controlled biophysically by the different plant growth and mortality rates associated with

12   herbaceous vegetation and shrubs. While grasses and forbs are associated with high rates of

13   plant growth and mortality, shrubs are associated with comparatively lower plant growth and

14   mortality rates (Ogle and Reynolds, 2004; Gilad et al., 2007).

15   We use a simplified version of the dynamic ecohydrological model developed by Rietkerk et

16   al. (2002) to illustrate conceptually how the vegetation-specific rates of plant growth and

17   mortality control the relationship between the dynamics of aboveground biomass and

18   antecedent rainfall for herbaceous vegetation and shrubs in drylands. The model consists of

19   two interrelated differential equations; one describing the dynamics of vegetation

20   (aboveground green biomass, B, g m^{-2}) and the other describing soil-moisture dynamics (soil-

21   water availability, W, mm).

22   Changes in plant biomass are controlled by plant growth and mortality:

23   $$\frac{dB}{dt} = g_{max} \frac{W - W_0}{W + k_w} B - mB, \qquad\qquad (1)$$

24   where plant growth is a saturation function of soil-moisture availability, and is determined by

25   the maximum specific plant-growth rate (g_{max}, day^{-1}), the permanent wilting point or

26   minimum availability of soil moisture for vegetation growth (W_0, mm), and a half saturation

27   constant (k_w, mm). Plant senescence (biomass loss) is controlled by a plant-specific mortality

28   coefficient (m, day^{-1}).

29   Soil-water dynamics are controlled by rainfall infiltration, plant transpiration, and soil-

30   moisture loss due to both deep drainage and direct evaporation:

1   $$\frac{dW}{dt} = P\frac{B+k_i \cdot i_0}{B+k_i} - cg_{max}\frac{W-W_0}{W+k_w}B - r_w W, \qquad\qquad (2)$$

2   where water infiltration is modelled as a saturation function of plant biomass, characterized

3   by the minimum proportion of rainfall infiltration in the absence of vegetation (i_0,

4   dimensionless), a half saturation constant (k_i, g m^{-2}) and daily precipitation (P, mm day^{-1}).

5   Plant transpiration is controlled by plant growth, and is modulated by a plant-water-

6   consumption coefficient (c, l g^{-1}). Finally, water losses to both deep drainage and direct

7   evaporation are modeled as a linear function of soil-water availability, with a rate r_w (day^{-1}).

8   A Maple 9.5 (Maplesoft, Waterloo, Canada) code for this model is available for download as

9   online supporting material of this article (Code 1).

10   Two sets of plant-growth and mortality coefficients were applied to this model to simulate

11   vegetation dynamics for a herbaceous species (g_{max}=0.32 day^{-1}, m=0.05 day^{-1}) and a shrub

12   (g_{max}=0.12 day^{-1}, m=0.03 day^{-1}), following criteria established in previous studies (Ogle and

13   Reynolds, 2004; Gilad et al., 2007). Plant-biomass dynamics for these two vegetation types

14   (Fig. 1a) were modelled using a north Chihuahuan Desert 15-year daily precipitation series

15   obtained at the Sevilleta National Wildlife Refuge (Sevilleta LTER,

16   http://sev.lternet.edu/data/sev-1; mean annual rainfall 238 mm) and a set of parameters

17   obtained from literature suited to dryland environments: W_0= 0.05 mm, k_w= 0.45 mm,

18   k_i = 180 g m^{-2}, i_0= 0.20, c= 0.1 l g^{-1}, r_w= 0.1 day^{-1} (Rietkerk et al., 2002; Gilad et al., 2007;

19   Saco and Moreno-de las Heras, 2013).

20   Using this model, we explored the strength of the plant biomass-precipitation relationship as a

21   function of the length of rainfall accumulation (Fig 1b). We have applied Pearson's R

22   correlation between the simulated plant biomass for both the herbaceous and the shrub species

23   and antecedent rainfall series using various lengths of rainfall accumulation; i.e. for any time

24   t_i in the plant biomass series, the rainfall in the preceding day (t_{i-1}), the cumulative rainfall in

25   the two preceding days ($t_{i-1:i-2}$), in the three preceding days ($t_{i-1:i-3}$) and so on. Modelling

26   results show that the plant biomass-rainfall correlation is maximized at 52 days of cumulative

27   rainfall for the simulated herbaceous species (Olr_{hv} = 52 days) and is maximized at 104 days

28   of cumulative rainfall for the modeled shrub species (Olr_s = 104 days; Fig. 1b). This result

29   indicates that the simulated herbaceous species responds to short-term (~ two months)

30   antecedent rainfall for the production of plant biomass whilst the simulated shrub species

31   responds to a longer period of antecedent precipitation to support plant dynamics. Here,

1   *ARain*$_{hv}$ and *ARain*$_s$ are defined as the antecedent rainfall series that optimize those

2   vegetation-type specific relationships (i.e. time series of precedent rainfall with accumulation

3   lengths *Olr*$_{hv}$ for herbaceous vegetation and *Olr*$_s$ for shrubs, Fig. 1a). Further analysis using a

4   range of plausible values for the plant-mortality and maximum plant-growth coefficients (Fig.

5   1c) indicates that *Olr* increases largely by reducing the characteristic plant-mortality and

6   growth rates of vegetation, and therefore suggests a strong influence on vegetation type.

7   Sensitivity analysis of *Olr* to other model parameters (Supplementary Fig.1 in the online

8   supporting information of this study) indicates that W_0, k_w, k_i, and c have negligible effects on

9   simulated *Olr* values. Reductions on bare soil infiltration (i_0) and increases on water loss by

10   direct evaporation and/or deep drainage (r_w) can impact *Olr*$_{hv}$ and *Olr*$_s$ values, ultimately

11   amplifying the differences we obtained between vegetation types. Other factors not explicitly

12   considered in our model, such as differences in root structure, may also reinforce herbaceous

13   and shrub differences in time-scale plant responses to antecedent precipitation (Reynolds et

14   al., 2004; Collins et al., 2014).

15   The simple model presented in this study provides a good starting point for addressing general

16   differences in plant responses to antecedent precipitation for different vegetation types in

17   drylands. Overall, our modelling results illustrate conceptually the distinct dependence of the

18   relationship between plant biomass and antecedent precipitation on vegetation type,

19   particularly when comparing the dynamics of dryland herbaceous and shrub vegetation.

20   In the following part of this study, we empirically determine and use metrics of reference

21   vegetation-type specific relationships between aboveground green biomass and antecedent

22   rainfall (i.e. optimal *Olr*$_{hv}$ and *Olr*$_s$ lengths, and corresponding *ARain*$_{hv}$ and *ARain*$_s$ series) to

23   explore the spatial organization and NPP dynamics of herbaceous and shrub vegetation at a

24   semi-arid grassland-shrubland ecotone.

25

26   **3   Materials and methods**

27   **3.1 Study area**

28   This study is conducted in the Sevilleta National Wildlife Refuge (SNWR), central New

29   Mexico, USA, the location of the Sevilleta Long Term Ecological Research (LTER) site. The

30   SNWR is located in the northern edge of the Chihuahuan Desert, and is a transition zone

31   between four major biomes: the Chihuahuan Desert, the Great Plains grasslands, the Colorado

1 Plateau steppe, and the Mogollon coniferous woodland (Fig. 2a). Livestock grazing has been

2 excluded from the SNWR since 1973, following 40 years of rangeland use. Due to the biome-

3 transition nature of the SNWR, minor variations in environmental conditions and/or human

4 use can result in large changes in vegetation composition and distribution at the refuge

5 (Turnbull et al., 2010b). Analysis of aerial photographs and soil-carbon isotopes indicate that

6 the extent of desert shrublands has considerably increased over the grasslands in regions of

7 the SNWR over the last 80 years (Gosz, 1992; Turnbull et al., 2008).

8 Our study area is an 18 km^2 grassland-shrubland ecotone within the McKenzie Flats, an area

9 of gently sloping terrain on the eastern side of the SNWR (Fig. 2b). This study area extends

10 over two LTER Core Sites established in 1999 (Fig. 2c): a desert shrubland (Creosotebush

11 SEV LTER Core Site) dominated by creosotebush, and a grassland (Black Grama SEV LTER

12 Core Site) dominated by black grama. The central and northeastern parts of the study area are

13 mixed black and blue grama (*Bouteloua eriopoda* and *B. gracilis*, respectively) grasslands.

14 The abundance of creosotebush (*Larrea tridentata*) in the grasslands is generally low,

15 although smaller shrubs and succulents (e.g. *Gutierrezia sarothrae*, *Ephedra torreyana*, *Yucca*

16 *glauca*, *Opuntia phaeacantha*) can be common. The abundance of perennial grass species

17 decreases to the southern and southwestern parts of the study area, where creosotebush stands

18 are widely distributed with in general low (although variable in time) amounts of annual forbs

19 and grasses. Soils are Turney sandy loams (Soil Survey Staff, 2010) with about 60% sand and

20 20% silt content (Muldavin et al., 2008; Turnbull et al., 2010b). The climate is semi-arid, with

21 mean annual precipitation of ~240 mm that is made up of 57% falling in the form of high-

22 intensity convective thunderstorms during the summer monsoon (June to September) and the

23 remainder being received as low-intensity frontal rainfall and snow (October to May). Mean

24 annual daily temperature is 14°C, with a winter average of 6°C and a summer average of

25 24°C. Daily air temperature rises over 10°C in the beginning of April, leading to the onset of

26 the yearly cycles of vegetation growth (Weiss et al., 2004). Vegetation growth in the study

27 area generally peaks between July and September, coinciding with the summer monsoon

28 (Muldavin et al., 2008).

29 **3.2 Vegetation measurements (remote sensed and ground based) and rainfall**
30   **data**

31 We use temporal series of NDVI as a proxy of aboveground green biomass in our study area.

32 NDVI is a remote-sensed chlorophyll-sensitive vegetation index that correlates with green

1 biomass in semi-arid environments (Anderson et al., 1993; Huete et al., 2002; Veron and

2 Paruelo, 2010). Differences in soil background brightness can generate important

3 uncertainties in relating NDVI levels to dryland vegetation, especially when vegetation cover

4 is low and soil type is heterogeneous in space (Okin et al., 2001). Despite these uncertainties,

5 multiple studies have demonstrated the usefulness of NDVI for examining primary production

6 and vegetation structure in arid and semi-arid ecosystems (for example, Weiss et al., 2004;

7 Choler et al., 2010; Moreno-de las Heras et al., 2012), and particularly in Chihuahuan

8 landscapes with sparse vegetation (30-50% cover) similar to those included in this study

9 (Peters and Eve, 1995; Peters et al., 1997; Pennington and Collins, 2007; Notaro et al., 2010).

10 We compiled decade-scale (2000-13) series of NDVI with a 16-day compositing period from

11 the MODIS Terra satellite (MOD13Q1 product, collection 5, approx. 250 m resolution). We

12 used the NASA Reverb search tool (NASA EOSDIS, http://reverb.echo.nasa.gov/) to

13 download the corresponding MODIS tiles. The data were re-projected to UTM WGS84 and

14 further resampled to fit our 18-km^2 study area (335 pixels; 231.5 m pixel resolution after re-

15 projection to UTM coordinates). We checked the reliability layer of the acquired MODIS

16 products and discarded those NDVI values that did not have the highest quality flag value

17 (less than 1 % of data). Missing values were interpolated using a second order polynomial. To

18 reduce inherent noise, the NDVI time series were then filtered by applying a Savitzky-Golay

19 smoothing algorithm, as recommended by Choler et al. (2010).

20 To validate remote sensing analysis of the spatial distribution of vegetation types, the

21 dominance of herbaceous vegetation, shrubs, perennial grass, forbs, and creosotebush plants

22 was recorded at a set of 27 control points (Fig. 2c) using the point-intercept method (Godin-

23 Alvarez et al., 2009). Vegetation presence/absence of the aforementioned vegetation types

24 was recorded every metre using a 2-cm diameter, 1.2-m tall, metal rod pointer along five 50-

25 m long linear transects that were laid at each control point at random directions (without

26 overlapping). Dominance was determined as the relative abundance of a particular vegetation

27 type in relation to the total amount of vegetated points found per linear transect.

28 Reference information on aboveground net primary production (NPP) was obtained from a

29 pre-existing, decade-scale (2000-11) dataset (Sevilleta LTER, http://sev.lternet.edu/data/sev-

30 182). This dataset was recorded in a set of 10 sampling webs distributed within the Black

31 Grama and Creosotebush SEV LTER Core Sites (five webs per Core Site, Fig. 2c). Each

32 sampling web consisted of four 25-m^2 square sub-plots located in each cardinal direction

around the perimeter of a 200-m diameter circle, with four 1-m^2 quadrats spatially distributed in the internal corners of the 25-m^2 sub-plots. A detailed description of the methods that were applied for the development of the SEV LTER field NPP dataset can be found in Muldavin et al. (2008). Briefly, species-specific plant standing biomass was estimated three times per year (in February-March, May-June and September-October) using allometric equations, and NPP was calculated seasonally for spring (the difference in plant biomass form March to May), summer (from June to September), and fall/winter (from October to February). For this study, we have used lumped records of annual net primary production (ANPP) for herbaceous vegetation and shrubs that were spatially averaged at the Core Site scale. ANPP for each yearly cycle of vegetation growth has been calculated as the sum of the seasonal NPP records (i.e. spring + summer + fall/winter).

Daily rainfall information for this study was obtained from an automated meteorological station located in the study site (the Five Points weather station, SEV LTER, Fig. 2c; Sevilleta LTER, http://sev.lternet.edu/data/sev-1). The meteorological station is equipped with a rain gauge that records precipitation on a 1-minute basis during periods of rain.

3.3 Reference NDVI-rainfall metrics for herbaceous vegetation and shrubs

We explored reference NDVI-rainfall relationships for herbaceous vegetation and shrubs in the Black Grama and Creosotebush SEV LTER Core Sites (where vegetation is dominantly herbaceous and shrub, respectively) using the 2000-13 NDVI time series (averaged from five MODIS pixels in each site, covering a total of 1200 m^2 per site). Pearson's correlations between NDVI and antecedent precipitation series were calculated for the two sites using various lengths of rainfall accumulation (1-300 days). Optimal length of rainfall accumulation for herbaceous vegetation and shrubs (Olr_{hv} and Olr_s, respectively) were then determined as the length of rainfall accumulation (in days) of the antecedent precipitation series that maximized the correlations between NDVI and rainfall in the black grama- and the creosotebush-dominated Core Sites, respectively. Growth of non-dominant herbaceous vegetation in arid shrublands can make the detection of shrub-specific NDVI-rainfall metrics (i.e. Olr_s) difficult due to the emergence of secondary Olr_{hv} values, particularly in wet years with strong herbaceous production (Moreno-de las Heras et al., 2012). We applied detailed analysis of the NDVI-rainfall relationships in the Core Sites for each annual cycle of vegetation growth to facilitate discrimination of the Olr_{hv} and Olr_s metrics. Our approach assumes linearity between rainfall and both NDVI values and green biomass, which has been

1 broadly demonstrated to occur for dryland vegetation (Evans and Geerken, 2004; Choler et

2 al., 2010; Notaro et al., 2010; Veron and Paruelo, 2010; Moreno-de las Heras et al., 2012) and

3 particularly in our grassland-shrubland desert ecotone (Pennington and Collins, 2007;

4 Muldavin et al., 2008).

5 The optimal antecedent rainfall series determined in the Core Sites for herbaceous vegetation

6 ($ARain_{hs}$, with Olr_{hv} length of rainfall accumulation) and shrubs ($ARain_s$, with Olr_s rainfall

7 accumulation length) were further used in our 18-km^2 ecotone to classify landscape types and

8 to decompose local NDVI signals into greenness components for herbaceous and shrub

9 vegetation.

10 **3.4   Spatial distribution of vegetation types and landscape classification**

11 We applied analysis of the relationship between local series of NDVI and the reference

12 $ARain_{hv}$ and $ARain_s$ antecedent rainfall series to determine the spatial distribution of dominant

13 vegetation and classify landscape types over our 18-km^2 ecotone study area. This analysis

14 builds on the assumption that spatial variations in the NDVI-rainfall relationship reflect

15 spatial differences in the dominance of vegetation types. We assume that areas dominated by

16 herbaceous vegetation (or shrubs) will show a strong NDVI-rainfall relationship for the

17 herbaceous-characteristic $ARain_{hv}$ (or the shrub-characteristic $ARain_s$) antecedent rainfall

18 series along the study period.

19 The strength of the relationship between NDVI and rainfall (quantified using Pearson's R

20 correlation between NDVI and antecedent precipitation) was calculated for every MODIS

21 pixel in the study area using the reference $ARain_{hv}$ and $ARain_s$ antecedent rainfall series.

22 Correlation values were determined for each cycle of vegetation growth (April-March) in

23 2000-13. In order to reduce data dimensionality, we applied Principal Component Analysis

24 (PCA) using the calculated correlation coefficients as variables for analysis (28 variables

25 resulting from the two vegetation-specific antecedent rainfall series and the 14 growing

26 cycles). We studied further the relationship between the main PCA factors and ground-based

27 dominance of vegetation types using the reference vegetation distribution dataset (27 control

28 points). Finally, we used the empirical relationships between vegetation dominance and the

29 main PCA factors to discriminate differentiated landscape types across the study area: grass-

30 dominated (GD), grass-transition (GT), shrub-transition (ST) and shrub-dominated (SD)

31 landscapes.

3.5 NDVI decomposition and transformation into herbaceous and shrub ANPP components

Time series of NDVI at any specific location reflects additive contributions of background soil and the herbaceous and woody shrub components of vegetation (C_{bs}, C_{hv}, and C_s, respectively) for that particular site (Lu et al., 2003):

$$NDVI(t) = C_{bs}(t) + C_{hv}(t) + C_s(t),\qquad(3)$$

Montandon and Small (2008) carried out *in situ* measurements of field spectra convolved by the MODIS bands to determine the background soil contribution to NDVI in the SNWR. They obtained a soil NDVI value of 0.12 for Turney sandy loam soils, which are broadly distributed across the McKenzie Flats. Analysis of the local MODIS NDVI time series revealed that this soil-background reference value broadly matches the minimum NDVI values for our study area. Application of reference soil values in NDVI decomposition and normalization methodologies provides an efficient standardization approach for characterizing the background soil baseline, particularly in areas with homogeneous soils (Carlson and Ripley, 1997; Roderick et al., 1999; Lu et al., 2003; Choler et al. 2010). Soil background NDVI may change with soil-moisture content (Okin et al., 2001). Although this effect can be especially important for dark organic-rich soils, soil-moisture variations have shown a little impact in desert-type bright sandy and sandy-loam soils, as those represented in the study area (Huete et al., 1985). Therefore, a constant value of 0.12 was applied to subtract the background soil baseline (C_{bs}) from the NDVI time series, obtaining a new set of soil-free series ($NDVI_O$):

$$NDVI_O(t) = C_{hv}(t) + C_s(t),\qquad(4)$$

We applied the reference herbaceous- and shrub-characteristic antecedent rainfall series, $ARain_{hv}$ and $ARain_s$, to partition single time series of soil-free NDVI ($NDVI_O$) into separate contributions for herbaceous vegetation (C_{hv}) and woody shrubs (C_s) across our study area. This approach is based on the assumption that the primary determinant of the dynamics of both NDVI and green biomass in Chihuahuan landscapes is the rainfall pattern (Huenneke et al., 2002; Weiss et al., 2004; Muldavin et al., 2008; Pennington and Collins, 2007; Notaro et al., 2010; Forzieri et al., 2011), and therefore the partial contributions of herbaceous vegetation and shrubs to NDVI can be estimated as a function of their characteristic dependency on antecedent rainfall. In other words, we assume that C_{hv} and C_s for any t_i are

1   proportional to $ARain_{hv}$ and $ARain_s$. The NDVI components for herbaceous vegetation and

2   shrubs were partitioned using the following two-step NDVI-decomposition procedure (Maple

3   9.5 code for analysis provided as online supporting material of this article; Code 2).

4   First, we applied first-order least-squares optimization of the relationship between soil-free

5   NDVI ($NDVI_O$) and the vegetation-type specific antecedent rainfall series ($ARain_{hv}$ and

6    $ARain_s$ for herbaceous vegetation and shrub, respectively):

7    $$NDVI_O(t) = h\,ARain_{hv}(t) + s\,ARain_s(t), \tag{5}$$

8   where, h and s represent vegetation-type specific rainfall-NDVI conversion coefficients for

9   the herbaceous and shrub components.

10   Secondly, we used the determined coefficients h and s to calculate the weights of C_{hv} and C_s

11   on the time series (i.e. the predicted percentage contribution of each vegetation type over the

12   predicted totals for any t_i). Seasonal variations in other environmental factors (e.g.

13   temperature, day length) may influence NDVI dynamics for Chihuahuan vegetation, shaping

14   the responses of vegetation to precipitation (Weiss et al., 2004; Notaro et al., 2010). In order

15   to preserve the observed seasonality of the original NDVI time series in the decomposed

16   signals for herbaceous and shrub vegetation, the predicted weights (or percentage

17   contributions) of the fitted vegetation components were reassigned to the NDVI levels of the

18   original time series, obtaining the final NDVI components for herbaceous vegetation and

19   shrubs (C_{hv}, and C_s, respectively). Computed soil background baseline, C_{bs}, plus the

20   partitioned NDVI components for herbaceous vegetation, C_{hv}, and shrubs, C_s, total the

21   original NDVI levels of the temporal series for any point in time and space.

22   The 2000-13 time series of NDVI were decomposed into separate contributions of herbaceous

23   vegetation and shrubs for the Black Grama and Cresotebush SEV LTER Core Sites. We used

24   the reference 2000-11 field NPP dataset to study the relationship between the decomposed

25   NDVI time series and ground-based estimates of herbaceous and shrub NPP for the Core

26   Sites. The sum of the herbaceous and the shrub NDVI components ($\sum NDVI_{veg.type}$) were

27   calculated for each growing cycle of vegetation (April-March). We further determined the

28   relationships between field ANPP estimates of herbaceous and shrub vegetation and

29    $\sum NDVI_{veg.type}$. Finally, we applied the signal-decomposition procedure to every single NDVI

30   time series of the 335 MODIS pixels contained within our study area. The established Core

1 Site NDVI-ANPP relationships were used to estimate herbaceous and shrub ANPP across the

2 18 km^2 study site.

3.6 Spatiotemporal dynamics of vegetation production and impact of seasonal precipitation on herbaceous and shrub ANPP

5 We used the remotely sensed ANPP estimations and landscape-type classification (GD, grass-

6 dominated, GT, grass-transition, ST, shrub-transition, and SD, shrub-dominated landscapes)

7 to analyze the spatiotemporal dynamics of ANPP along our study grassland-shrubland

8 ecotone, applying repeated-measures ANOVA with time as within subjects factor and

9 landscape type as between subjects factor. Departures from sphericity were corrected using

10 the Greenhouse-Geisser F-ratio method for repeated-measures ANOVA (Girden, 1992).

11 2000-13 activity of the shrub-encroachment phenomenon for the established landscape types

12 (GD, GT, ST and SD) was explored applying Pearson's R correlation between shrub

13 contribution to total ANPP and time.

14 We used three different seasonal precipitation metrics to analyze the impact of inter-annual

15 variations in seasonal precipitation on the production of herbaceous and shrub vegetation at

16 our ecotone: (i) preceding non-monsoonal rainfall (Rain$_{PNM}$, from October to May) that takes

17 place before the summer peak of vegetation growth, (ii) summer monsoonal precipitation

18 (Rain$_{SM}$, from June to September), and (iii) late non-monsoonal rainfall (Rain$_{LNM}$, from

19 October to March) that takes place at the end of the annual cycles of vegetation growth. The

20 effects of seasonal precipitation on herbaceous and shrub ANPP for the established landscape

21 types (grass-dominated, grass-transition, shrub-transition and shrub-dominated landscapes)

22 were explored by applying Pearson's R correlation. Effect significance and size was

23 determined using a general linear model (GLM) that includes the different sources of seasonal

24 precipitation (Rain$_{PNM}$, Rain$_{SM}$, and Rain$_{LNM}$) as covariates, landscape type (LT) as a factor,

25 and the interaction terms between landscape type and seasonal precipitation (LT:Rain$_{PNM}$,

26 LT:Rain$_{SM}$, and LT:Rain$_{LNM}$).

27

4 Results

4.1 Patterns of greenness and reference NDVI-rainfall metrics in the Core Sites

Inter- and intra-annual variations of NDVI show similar patterns of vegetation greenness for both the Black Grama and the Creosotebush Core Sites (Fig. 3a). The signal generally peaks slightly in spring (May) and strongly in summer (July-September). The lowest NDVI values are observed between February and April. Summer peaks in NDVI values are, however, less marked in the Creosotebush Core Site. In addition, the NDVI signal for the creosotebush-dominated site generally shows an autumn (October-November) peak that is especially important during particular growing cycles (2000-01, 2001-02, 2004-05, 2007-08, 2009-10).

Correlations between NDVI and antecedent precipitation using rainfall-accumulation lengths of 1-300 days indicate that an optimal short-term cumulative rainfall period of 57 days best explains the NDVI variations for the dominant herbaceous vegetation of the grassland site ($ARain_{hv}$ antecedent rainfall series, with Olr_{hv} accumulation length; Fig. 3, see also Supplementary Fig. 2 in the online supporting information of this study for details on the annual cycles of vegetation growth). For the Creosotebush Core Site (with dominant shrub vegetation and subordinate forbs and grasses), the short-term, 57-day antecedent rainfall series $ARain_{hv}$ also has an important impact on the strength of the NDVI-rainfall relationship, particularly for three consecutive growing cycles with strong summer precipitation (2006-07, 2007-08 and 2008-09, summer precipitation for the period is 40% above the long-term mean). However, the NDVI-rainfall correlation in this shrub-dominated site generally peaks using a much longer optimal cumulative rainfall period of nearly 145 days ($ARain_{s}$ series, with Olr_{s} length).

4.2 Spatial distribution of vegetation types and landscape classification

PCA analysis of the NDVI-rainfall correlation coefficients (per growing cycle) for the reference 57- and 145-day antecedent rainfall series (i.e. $ARain_{hv}$ and $ARain_{s}$ with Olr_{hv} and Olr_{s} rainfall accumulation lengths, respectively for all MODIS pixels contained within our study area) shows that PCA factor 1 (about 40% of total data variance) reflects a landscape gradient that discriminates the two reference responses of vegetation greenness to antecedent rainfall (Figs. 4a and 4b). The correlation between the NDVI and the short-term antecedent

1   rainfall series *ARain$_{hv}$* increases to the negative side of factor 1 (particularly for growing

2   cycles 2001-02, 2002-03, 2005-06, and 2012-13), while the correlation with the 145-day

3   antecedent rainfall series (*ARain$_s$*) increases to the positive side of the this factor (particularly

4   for cycles 2000-01, 2002-03, 2005-06, and 2006-07, Fig. 4b). Analysis of the relationship

5   between PCA factor 1 and vegetation dominance for the ground-based set of control points

6   indicates that this landscape gradient is explained by the field distribution of dominant

7   vegetation types since the dominance of herbaceous vegetation and shrubs increases to the

8   negative and positive side of PCA factor 1, respectively (R^2 approx. 0.90, Fig. 4c).

9   Four different landscape types (GD, GT, ST and SD) are defined in the 18-km^2 study area as

10   determined by the spatial projection of the relationship between PCA factor 1 and field

11   dominance of herbaceous and shrub vegetation (Figs. 4c and 4d). SD, ST and GT landscapes

12   are distributed in the southwestern part of the study site, while GD landscapes are located in

13   the central and northeastern parts of the area (Figs. 4d and 4e).

4.3   NDVI transformation into herbaceous and shrub ANPP components

14

15   Temporal decomposition of NDVI into partial herbaceous and shrub vegetation components

16   results in very different outputs for the reference Black Grama and Creosotebush Core Sites

17   (Fig. 5a). The herbaceous component (which is derived from the relationship between NDVI

18   and the reference 57-day antecedent rainfall series, *ARain$_{hv}$*) prevails in the grass-dominated

19   reference site, whilst the shrub component (which is function of the reference 145-day

20   antecedent rainfall series, *ARain$_s$*) comprises the leading NDVI fraction in the shrub-

21   dominated reference site.

22   The annual sums of herbaceous and shrub NDVI components for the reference Core Sites

23   show a strong linear agreement ($R^2 \geq 0.65$; $P<0.001$) with ground-based measurements of

24   ANPP (Fig. 5b) , while the remote-sensing ANPP estimations yield a root mean square error

25   of 26 g m^{-2} (NRMSE 12%, Fig. 5c).

26   Spatial projection of the reference NDVI-ANPP relationships across the 18 km^2 study area

27   displays a contrasted distribution of mean 2000-13 ANPP for herbaceous and shrub

28   vegetation (Figs. 5d and 5e). Herbaceous ANPP is mainly distributed in the central and

29   northeastern parts of the study site, contributing to >80% total ANPP. Conversely, shrub

30   ANPP is concentrated in the southwestern edge of the study area.

4.4 ANPP spatiotemporal dynamics and impact of seasonal precipitation on herbaceous and shrub primary production

Remote-sensed estimations of ANPP are significantly impacted by landscape type ($F_{3, 334}$=48.6, P<0.01), with grass-dominated sites supporting in general higher levels of vegetation production (Fig. 6a). However, landscape-type effects are variable in time (landscape type x time interaction: $F_{14, 1515}$=57.2, P<0.01). Year-to-year variability of ANPP is particularly large for the grass-dominated sites, which show higher levels of ANPP than the transition and shrub-dominated landscapes for highly productive years (Fig. 6a). For growing cycles with low primary production there are no significant ANPP differences or the differences are reversed, with shrub-dominated sites showing higher production than grass-dominated sites (e.g. 2003-04 cycle, Fig. 6a).

Analysis of the temporal evolution of shrub contribution to total ANPP along 2000-13 reflects significant (although very weak) positive correlations with time for the grass- and shrub transition landscapes (Fig. 6b). The same analysis at the individual pixel level, however, does not show any significant correlations between shrub contribution to total ANPP and time.

Exploratory analysis of the influence of seasonal precipitation on remote-sensed estimations of ANPP indicates different responses for herbaceous and shrub vegetation (Fig. 7). Herbaceous ANPP strongly correlates with monsoonal summer precipitation for all landscape types (Fig. 7a). The slope of the relationship between herbaceous ANPP and monsoonal summer (June-September) precipitation decreases for the shrub-transition and shrub-dominated landscapes. Conversely, shrub ANPP strongly correlates with both preceding non-monsoonal (October-May) and monsoonal summer (June-September) precipitation for all landscape types (Fig. 7b).

General linear model results confirm the exploratory observations of the relationships between remote-sensed estimations of ANPP and seasonal precipitation (Table 1). Model results identify both monsoonal summer precipitation (Rain$_{SM}$) and the interaction between Rain$_{SM}$ and landscape type as the most important contributors (effect size, $\eta^2 > 10\%$; P<0.001) to the total variance comprised in ANPP data for herbaceous vegetation. Similarly, non-monsoonal summer precipitation (Rain$_{PNM}$) and monsoonal summer precipitation (Rain$_{SM}$) are identified as the leading contributors to shrub ANPP.

5   Discussion

5.1   Vegetation-growth pattern and reference NDVI-rainfall metrics for herbaceous and shrub vegetation

Analysis of time series of NDVI provides important information on the dynamics of vegetation growth in drylands (Peters et al., 1997; Holm et al., 2003; Weiss et al., 2004; Choler et al., 2010). NDVI trends in the grass-dominated site show strong peaks centered in the summer season (Fig. 3a), which agrees with both field and remote-sensed observations of the dynamics of aboveground biomass for desert grasslands dominated by *Bouteoula eriopoda* and *B. gracilis* in the area (Peters and Eve, 1995; Huenneke et al., 2002; Muldavin et al., 2008; Notaro et al., 2010). For the shrub-dominated site, summer peaks in the NDVI signal are smaller, and for particular years both spring and late-autumn peaks can exceed summer greenness. Accordingly, the timing of plant growth for *Larrea tridentata* (which dominates the reference shrubland site) has been shown to vary from year to year, since this species has the ability to shift the temporal patterns of vegetation growth to take advantage of changes in resource availability (Fisher et al., 1988; Reynolds et al., 1999; Weiss et al., 2004; Muldavin et al., 2008).

The analysis of the relationships between NDVI and precipitation provide further insights on plant water-use patterns and, hence, on vegetation function and structure (Pennington and Collins, 2007; Veron and Paruelo, 2010; Notaro et al., 2010; Garcia et al., 2010; Forzieri et al., 2011; Moreno-de las Heras et al., 2012). Temporal trends in NDVI for the reference grass- and shrub-dominated SEV LTER sites are explained by antecedent (or preceding cumulative) rainfall amounts, reflecting the coupling of the history of plant-available soil moisture with vegetation growth (Fig. 3). Correlations between NDVI and precipitation indicate that plant growth pulses for the grass-dominated site are associated with short-term antecedent rainfall ($ARain_{hv}$ series; 57 days optimal length, Olr_{hv}). For the shrub-dominated landscape, vegetation greenness shows a strong association with longer-term antecedent precipitation ($ARain_s$ series; 145 days optimal length, Olr_s), although importantly, NDVI dynamics for this site also correlate with the 57-day cumulative rainfall series. Previous work on the analysis of NDVI-rainfall relationships found similar variations in the length of the antecedent rainfall series that best explain the dynamics of vegetation greenness, suggesting that such differences result from site variations in dominant vegetation (Evans and Geerken, 2004; Prasad et al., 2007; Garcia et al., 2010).

1   Given the strong relationship between time-integrated NDVI values and ground-based ANPP

2   estimations for our site (Fig. 5b), our herbaceous and shrub exploratory modeling results

3   provide a biophysical explanation for the range of variations found in the NDVI-rainfall

4   relationships (Fig. 1). The length of the cumulative precipitation series that optimizes the

5   relationship between plant biomass and antecedent rainfall (Olr) appears to be a function of

6   the characteristic water-use and plant growth pattern of dryland vegetation, that are largely

7   influenced by the plant-growth and mortality rates of vegetation (Fig. 1c). Vegetation growth

8   and water use strongly differ for herbaceous and shrub life-forms in drylands (Sparrow, 1997;

9   Ogle and Reynolds, 2004; Gilad et al., 2007; Garcia et al., 2010), in which case plant biomass

10 dynamics respond to short-term and long-term antecedent precipitation, respectively (Figs.

11 1a-b). Olr variations in the reference SEV LTER Core Sites may, therefore, be expressed as a

12 function of the dominant vegetation types (Fig. 3): the strong and quick responses of

13 greenness to short-term precipitation ($ARain_{hv}$) in the grass-dominated Black Grama Core Site

14 characterize herbaceous growth for the area, while the slow responses of NDVI to medium-

15 term precipitation ($ARain_s$) in the shrub-dominated Cresotebush Core Site define the

16 characteristic pattern of vegetation growth for shrubs in the ecotone. The high correlation

17 between $ARain_{hv}$ and NDVI values in the shrub-dominated Creosotebush Core Site (Fig. 3b)

18 can be explained by the growth of non-dominant herbaceous vegetation (mainly annual

19 forbs), which can be especially important during wet years (Muldavin et al., 2008; Baez et al.,

20 2012). Similarly, Moreno-de las Heras et al. (2012) in dry open-shrublands of central

21 Australia (Olr_s values about 220 days) found the emergence of secondary Olr_{hv} metrics on the

22 study of local NDVI-rainfall relationships (approx. 85 days antecedent rainfall length) caused

23 by the growth of non-dominant herbaceous vegetation. Overall, Olr values determined for

24 herbaceous and shrub vegetation in this work are in agreement with the range of characteristic

25 antecedent rainfall series reported in other studies to best describe green biomass dynamics

26 for arid and semi-arid grasslands (1-3 months) and woody shrublands (4-8 months) (Evans

27 and Geerken, 2004; Munkhtsetseg et al., 2007; Garcia et al., 2010; Moreno-de las Heras et al.,

28 2012).

29 **5.2 Spatial distribution and net primary production of herbaceous vegetation**
30   **and shrubs**

31 Our results indicate that the relationship between temporal series of remotely sensed NDVI

32 and antecedent precipitation is highly sensitive to spatial differences in dominant vegetation

1   (Fig. 4). The main PCA factor (explaining about 40% variance in data) extracted using the

2   annual NDVI responses (i.e. the Pearson's R coefficients) to the reference 57- and 145-day

3   characteristic antecedent rainfall series ($ARain_{hv}$ and $ARain_s$ series, respectively) accurately

4   discriminates the behavior of herbaceous and shrub vegetation for the 18 km^2 study area

5   (Figs. 4b-c), hence providing a robust approach for classifying landscapes as a function of the

6   dominance of vegetation types using coarse-grained remotely sensed data (Fig. 4d). This

7   parsimonious approach offers a practical alternative to other more complex remote-sensing

8   methodologies for the analysis of the spatial distribution of vegetation types in mixed

9   systems, such as Spectral Mixture Analysis (SMA, Smith et al., 1990), which may be difficult

10   to apply in this Chihuahuan case study since both the mixed nature and fine-grained

11   distribution of vegetation in the area (patches of grass and shrubs are typically <1 m^2 and 0.5-

12   5 m^2, respectively; Turnbull et al. 2010b) can impose serious drawbacks on the detection of

13   reference spectral signatures for pure herbaceous and shrub vegetation using coarse-grained

14   MODIS data. Implementing SMA-based approaches for the analysis of vegetation distribution

15   and landscape classification in drylands using medium- and coarse-grained data is very

16   challenging since it requires significant amounts of ancillary data (e.g. laboratory-based or

17   field multi-date spectra for vegetation types) to solve data uncertainties generated by surface

18   heterogeneity, which is often not feasible (Somers et al. 2011).

19   The relationships of vegetation greenness to $ARain_{hv}$ and $ARain_s$ also provide criteria for

20   decomposing and transforming the NDVI signal into structural components of primary

21   production for this study. Lu et al. (2003) applied seasonal trend decomposition to partition

22   NDVI into (cyclic) herbaceous and (trend) woody vegetation in Australia. They assumed a

23   long-term weak phenological wave and a strong annual response for determining the shrub

24   and herbaceous components of vegetation, respectively. Our approach relies on the use of

25   differences in biophysical properties of herbaceous and shrub vegetation related to the

26   coupling between vegetation growth and precipitation for decomposing the NDVI signal,

27   rather than apparent differences in the seasonality of vegetation greenness alone. As expected,

28   signal decomposition outcomes indicate that the herbaceous component of the NDVI leads the

29   temporal trends for the grass-dominated reference Black Grama Core Site, while the shrub

30   component largely dominates the NDVI signal for the Creosotebush Core Site (Fig. 5a).

31   Although affected by data dispersion, the annual sums of decomposed NDVI strongly agree

32   with field estimations of ANPP for herbaceous and shrub vegetation ($R^2 \geq 0.65$, Fig. 5b),

1   resulting in a small root mean square error for our remote-sensing ANPP estimates (26 g m^{-2},

2   NRMSE 12%, Fig 5c) that is within the lower limit of reported errors by other NDVI

3   decomposition studies (for example, Roderick et al., 1999; DeFries et al., 2000, Hansen et al.,

4   2002; Lu et al., 2003; with NRMSE ranging 10-17%). Other dryland studies have found

5   important levels of data dispersion when relating fine-grained field ANPP to coarse-scale

6   NDVI values (Lu et al., 2003; Holm et al., 2003; Pennington and Collins, 2007; Veron and

7   Paruelo, 2010). Major sources of data dispersion for this study are most likely associated with

8   the high spatial variability of ANPP in the analyzed systems. For instance, field estimations

9   have shown that ANPP for both grass- and shrub-dominated Chihuahuan landscapes are

10   affected by important levels of spatial variability, primarily due to the patchiness of

11   vegetation cover (Huenneke et al., 2002; Muldavin et al., 2008).

12 **5.3   Spatiotemporal dynamics of ANPP and impact of seasonal precipitation**

13 **on herbaceous and shrub primary production**

14   Cross-scale interactions between vegetation composition, individual plant characteristics and

15   climatic drivers (e.g. variations in precipitation amount and seasonality) have an important

16   role on determining primary production patterns in arid and semi-arid ecosystems (Peters,

17   2002; Snyder and Tartowsky, 2006; Pennington and Collins, 2007; Notaro et al., 2010; Baez

18   et al., 2013). Analysis of the spatiotemporal dynamics of ANPP in our ecotone indicates that

19   grass-dominated sites, although very importantly affected by year-to-year variability,

20   generally support higher primary production than transition and shrub-dominated landscapes,

21   particularly for wet years with high ANPP levels (Fig. 6a). This result is consistent with other

22   shrub-encroachment studies which have found associations between shrub proliferation and

23   ANPP reductions in dry American grasslands (Huenneke et al., 2002; Knapp et al., 2008).

24   Our results suggest that primary production is differently controlled by seasonal precipitation

25   for herbaceous and shrub vegetation across the 18-km^2 Chihuahuan Desert ecotone (Fig 7,

26   Table 1). Monsoonal summer precipitation (June-September) controls ANPP for herbaceous

27   vegetation (Fig. 7a), while ANPP for shrubs is better explained by the preceding year's non-

28   monsoonal (October-May) plus the summer monsoonal precipitation in the present year (Fig

29   7b). Accordingly, field observations of ANPP for Chihuahuan landscapes found that

30   grassland primary production is particularly coupled with monsoonal rainfall, while desert

31   shrublands appear to be less dependent on summer precipitation (Fisher et al., 1988; Reynolds

32   et al., 1999; Huenneke et al., 2002; Muldavin et al., 2008; Throop et al., 2012).

1   Differences in the distribution of rainfall types, soil-moisture dynamics, and rooting habits of

2   dominant plant species may explain the variable impact of seasonal precipitation on

3   herbaceous and shrub ANPP for the studied Chihuahuan landscapes. Monsoonal summer

4   precipitation (July-September, approx. 60% annual precipitation) generally takes place in the

5   form of high-intensity thunderstorms that infiltrate shallow soil depths (top 15-35 cm)

6   (Snyder and Tartowsky, 2006). Summer soil-water resources for plant production are

7   ephemeral and strongly affected by evapotranspiration, which typically reduces soil moisture

8   to pre-storm background levels in 4-7 days after rainfall (Turnbull et al., 2010a). C_4 grasses

9   (*Bouteloua eriopoda* and *B. gracilis*), which dominate herbaceous vegetation in the analyzed

10   ecotone, concentrate active roots in the top 30 cm of the soil and intensively exploit

11   ephemeral summer soil moisture for plant growth (Peters, 2002; Muldavin et al., 2008).

12   Preferential spatial redistribution of runoff to grass patches following summer storms further

13   enhances plant production for black and blue grama (Wainwright et al., 2000; Pockman and

14   Small, 2010; Turnbull et al., 2010b).

15   Non-monsoonal precipitation (about 40% annual precipitation, primarily from November to

16   February) typically falls in the form of long-duration low-intensity frontal rainfall that often

17   percolates to deep soil layers (Snyder and Tartowsky, 2006). *Larrea tridentata*, the dominant

18   C_3 shrub in the studied ecotone, has a bimodal rooting behavior that facilitates the use of both

19   shallow and deep soil moisture for plant production (Fisher et al., 1988; Reynolds et al., 1999;

20   Ogle and Reynolds, 2004). Deep creosotebush roots (70-150 cm depth) may acquire winter-

21   derived soil-water resources that are unavailable to grass species, while active roots near the

22   surface (20-40 cm depth) may serve to access summer-derived shallow soil moisture for plant

23   growth (Gibbens and Lenz, 2001). The observed reduction in summer rain-use efficiency of

24   herbaceous vegetation for the shrub-transition and shrub-dominated landscapes (i.e. variations

25   on the slope of the relationship between herbaceous ANPP and summer precipitation, Fig. 7a)

26   suggests competitive effects of creosotebush for the use of shallow water sources, probably

27   associated to the large spatial extent of near-surface active roots (the radial spread of which

28   typically ranges between 2-6 m, Gibbens and Lenz, 2001). Alternative, landscape changes

29   induced by shrub encroachment (i.e. increased runoff and erosion) may reduce the ability of

30   grass patches to capitalize on horizontal redistribution of runoff for plant growth after summer

31   storms (Wainwright et al., 2000; Turnbull et al., 2012; Stewart et al. 2014).

1 Conceptual and mechanistic models of vegetation change suggest that vegetation composition

2 in arid and semi-arid landscapes is likely to be highly sensitive to climate change, and point at

3 variations in the amount and distribution of precipitation as a major driver of shrub

4 encroachment into desert grasslands (Peters, 2002; Gao and Reynolds, 2003; Snyder and

5 Tartowsky, 2006). Overall our results agree with those findings and suggest that changes in

6 the amount and temporal pattern of precipitation comprising reductions in monsoonal summer

7 rainfall and/or increases in winter precipitation may enhance the encroachment of

8 creosotebush into desert grasslands dominated by black and blue grama. Analysis of long-

9 term rainfall series indicates that winter precipitation has increased during the past century in

10 the northern Chihuahuan Desert, particularly since 1950, probably associated with the more

11 frequent occurrence of ENSO events for that period (Dahm and Moore, 1994; Wainwright,

12 2006). This pattern of precipitation change may be responsible, at least in part, of past

13 increase in woody shrub abundance over desert grasslands in the American Southwest (Brown

14 et al., 1997; Snyder and Tartowsky, 2006; Webb et al., 2003). Our results suggest that shrub

15 encroachment has not been particularly active in the studied ecotone for 2000-13 (Fig. 6b).

16 Accordingly, Allen et al. (2008) in a recent study on creosotebush plant architecture and age

17 structure indicated that the most important pulses of shrub encroachment for this area took

18 place between 1950 and 1970. Precise estimation of shrub cover applying segmentation

19 methods in time series of high-resolution imagery could help to accurately determine the

20 intensity of the shrub-encroachment phenomenon under the present variability in precipitation

21 for our grassland-shrubland ecotone.

22 Climate-change projections for the area suggest a general picture of increased aridity in the

23 next 100 years, with increased evaporation due to higher summer temperatures, and increased

24 drought frequency (Christensen and Konikicharla, 2013). The capacity of *L. tridentata* to

25 switch between different soil-water sources (i.e. summer-derived ephemeral shallow soil

26 moisture and more stable deep soil-water reserves derived from winter rainfall) and adapt the

27 timing of vegetation growth to take advantage of changes in resource availability make this C_3

28 shrub less susceptible to predicted increases in aridity than C_4 grasses that are strongly

29 dependent on summer precipitation (Reynolds et al., 1999; Throop et al., 2012; Baez et al.,

30 2013). Current increases in atmospheric CO_2 concentrations may also contribute to reduce the

31 competitiveness of C_4 grasses for the use of soil-water resources against C_3 desert shrubs

32 (Polley et al., 2002). Remaining desert grasslands in the American Southwest may, therefore,

1 be increasingly susceptible to shrub encroachment under the present context of changes in

2 climate and human activities.

3

6 Conclusions

5 In this study we applied a new analytical methodology for the study of the organization and

6 dynamics of vegetation at a grassland-shrubland Chihuahuan ecotone with variable abundance

7 of grasses (primarily *Boutelua eriopoda* and *B. gracilis*) and shrubs (mainly *Larrea*

8 *tridentata*), based on the exploration of the relationship between time series of remote-sensed

9 vegetation greenness (NDVI) and precipitation. Our results indicate that the characteristics of

10 the NDVI-rainfall relationships are highly dependent on differences in patterns of water use

11 and plant growth of vegetation types. In fact, NDVI-rainfall relationships show a high

12 sensitivity to spatial variations on dominant vegetation types across the grassland-shrubland

13 ecotone, and provide ready biophysically based criteria to study the spatial distribution and

14 dynamics of net primary production (NPP) for herbaceous and shrub vegetation. The analysis

15 of the relationship between NDVI and precipitation offers, therefore, a powerful methodology

16 for the study of broad-scale vegetation shifts comprising large changes in the dominance of

17 vegetation types in drylands using coarse-grained remotely sensed data, and could be used to

18 target areas for more detailed analysis and/or the application of mitigation measures.

19 Analysis of remote-sensed NPP dynamics at the grassland-shrubland ecotone reflects a

20 variable performance of dominant vegetation types. Herbaceous production is synchronized

21 with monsoonal summer rainfall, while shrub NPP shows a flexible response to both summer

22 and winter precipitation. Overall our results suggest that changes in the amount and temporal

23 pattern of precipitation (i.e. reductions in summer precipitation and/or increases in winter

24 rainfall) may intensify the shrub-encroachment process in the studied desert grasslands of the

25 American Southwest, particularly in the face of predicted general increases in aridity and

26 drought frequency for the area.

27

References

Al-Bakri, J. T., and Suleiman, A. S.: NDVI response to rainfall in different ecological zones in Jordan, Int. J. Remote Sens., 10, 3897-3912, 2004.

Allen, A. P., Pockman, W. T., Restrepo, C., and Milne, B. T.: Allometry, growth and population regulation of the desert shrub Larrea tridentata, Funct. Ecol., 22, 197-204, 2008.

Anderson, G. L., Hanson, J. D., and Haas., R. H.: Evaluating Landsat Thematic Mapper derived vegetation indices for estimating above-ground biomass on semiarid rangelands, Remote Sens. Environ., 45, 165-175, 1993.

Baez, S., Collins, S. C., Pockman, W. T., Johnson, J. E., and Small, E. E.: Effects of experimental rainfall manipulations on Chihuahuan Desert grassland and shrubland plant communities, Oecologia, 172, 1117-1127, 2013.

Brown, J. H., Valone, T. J., and Curtin, C. G.: Reorganization of an arid ecosystem in response to recent climate change, P. Natl. Acad. Sci. USA., 94, 9729-9733, 1997.

Buffington, L. C., and Herbel, C. H.: Vegetational changes on a semidesert grassland range from 1858 to 1963, Ecol. Monogr., 35, 139-164, 1965.

Carlson, T. N., and Ripley, D. A.: On the relation between NDVI, fractional cover, and leaf area index, Remote Sens. Environ., 62, 241-252, 1997.

Choler, P., Sea, W., Briggs, P., Raupauch, M., and Leuning, R.: A simple ecohydrological model captures essentials of seasonal leaf dynamics in semiarid tropical grasslands, Biogeosciences, 7, 907-920, 2010.

Christensen, J. H, and Konikicharla, K. K.: Climate phenomena and their relevance for future regional climate change, in: Climate Change 2013: The Physical Science Basis, Contribution of

Working Group I to the Fifth Assessment Report of the Intergovernmental Panel on Climate Change, edited by: Stoker, T. F., Qin, D., Platter, G. K., Tignor, M., Allen, S. K., Boschung, J., Navels, A., Xia, Y., Bex, V., and Midgley, P. M., Cambridge University Press, Cambridge, UK, 1217-1308, 2013.

Collins, S. L., Belnap, J., Grimm, N. B., Rudgers, J. A., Dahm, C. N., D'Odorico, P., Litvak, M., Natvig, D. O., Peters, D. C., Pockman, W. T., Sinsabaugh, R. L., and Wolf, B. O.: A multiple, hierarchical model of pulse dynamics in arid-land ecosystems, Annu. Rev. Ecol. Evol. Syst., 45, 397-419, 2014.

Dahm, C. N., and Moore, D. I.: The El Niño/Southern Oscillation phenomenon and the Sevilleta Long-Term Ecological Research site, in: El Niño and Long-Term Ecological Research (LTER) Sites, edited by: Greenland, D., LTER Network Office, University of Washington, Seattle, USA, 12-20, 1994.

DeFries, R. S., Hansen, M. C., and Townshend, J. R.G.: Global continuous fields of vegetation characteristics: a linear mixture model applied to multiyear 8 km AVHRR data, Int. J. Remote Sens., 21, 1389-1414, 2000.

D'Odorico, P., Okin, G. S., and Bestelmeyer, B. T.: A synthetic review of feedbacks and drivers of shrub encroachment in arid grasslands, Ecohydrology, 5, 520-530, 2012.

Evans, J., and Geerken, R.: Discrimination between climate and human-induced dryland degradation, J. Arid Environ., 57, 535-554, 2004.

Fisher, F. M., Zak, J. C., Cunningham, G. L., and Whitford, W. G.: Water and nitrogen effects on growth and allocation patterns of creosotebush in the northern Chihuahuan Desert, J. Range Manage., 41, 387-391, 1988.

Forzieri, G., Castelli, F., and Vivoni, E. R.: Vegetation dynamics within the North American Monsoon Region, J. Climate, 24, 1763-83, 2011.

Gao, Q., and Reynolds, J. F.: Historical shrub-grass transitions in the northern Chihuahuan Desert: Modeling the effects of shifting rainfall seasonlity and event size over a landscape, Global Change Biol., 9, 1-19, 2003.

Garcia, M., Litago, J., Palacios-Orueta, A., Pinzon, J. E., and Ustin, S. L.: Short-term propagation of rainfall peturbations on terrestrial ecosystems in central California, Appl. Veg. Sci., 13, 146-162, 2010.

1 Gibbens, R. P., and Lenz, J. M.: Root systems of some Chihuahuan Desert plants, J. Arid
2 Environ., 49, 221-263, 2001.

3 Gilad, E., Shachak, M., and Meron, E.: Dynamics and spatial organization of plant
4 communities in water-limited systems, Theor. Popul. Biol., 72, 214-230, 2007.

5 Girden, E. R.: ANOVA: repeated measures, SAGE University Paper Series 7-84, SAGE
6 Publications, Newbury Park, USA, 1992.

7 Godin-Alvarez, H., Herrick, J. E., Mattocks, M., Toledo, D., and Van Zee, J.: Comparison of
8 three vegetation monitoring methods: their relative utility for ecological assessment and
9 monitoring, Ecol. Indic., 9, 1001-1008, 2009.

10 Gosz, J. R.: Ecological functions in a biome transition zone: translating local responses to
11 broad-scale dynamics, in: Landscape Boundaries: Consequences for Biotic Diversity and
12 Ecological Flows, edited by: Hansen, A. J., and di Castri, A. J., Springer, New York, USA, 56-
13 75, 1992.

14 Hansen, M. C., DeFries, R. S., Townshend, J. R. G., Sohlberg, R., Dimiceli, C., and Carroll,
15 M.: Towards an operational MODIS continuous field of percent tree cover algorithm: examples
16 using AVHRR and MODIS data, Remote Sens. Environ., 83, 303-319, 2002.

17 Holm, A. McR., Cridland, S. W., and Roderick, M. L.: The use of time-integrated NOAA
18 NDVI data and rainfall to assess landscape degradation in the arid and shrubland of Western
19 Australia, Remote Sens. Environ., 85, 145-158, 2003.

20 Huenneke, L. F., Anderson, J. P., Remmenga, M., and Schlesinger, W. H.: Desertification alters
21 patterns of aboveground net primary production in Chihuahuan ecosystems, Global Change
22 Biol., 8, 247-264, 2002.

23 Huete, A., Jackson, R. D., and Post, D. F.: Spectral response of a plant canopy with different
24 soil backgrounds, Remote Sens. Environ., 17, 37-53, 1985.

25 Huete, A., Didan, K., Miura, T., Rodriguez, E. P., Gao, X., and Ferreira, L. G.: Overview of the
26 radiometric and biophysical performance of the MODIS vegetation indices, Remote Sens.
27 Environ., 83,195-213, 2002.

28 Lu, H., Raupach, M. R., McVicar, T. R., and Barret, D. J.: Decomposition of vegetation cover
29 into woody and herbaceous components using AVHRR NDVI time series, Remote Sens.
30 Environ., 86, 1-16, 2003.

1 Millennium Ecosystem Assessment: Ecosystems and Human Well-being: Biodiversity

2 Synthesis, World Resources Institute, Washington, DC, USA, 2005.

3 Montandon, L. M., and Small, E. E.: The impact of soil reflectance on the quantification of the

4 green vegetation fraction from NDVI, Remote Sens. Environ., 112, 1835-1845, 2008.

5 Moreno-de las Heras, M., Saco, P. M., Willgoose, G. R., and Tongway, D. J.: Variations in

6 hydrological connectivity of Australian semiarid landscapes indicate abrupt changes in rainfall-

7 use efficiency of vegetation, J. Geophys. Res., 117, G03009, doi:10.1029/2011JG001839, 2012.

8 Mueller E. N., Wainwright, J., and Parsons, A. J.: The stability of vegetation boundaries and

9 the propagation of desertification in the American Southwest: A modelling approach, Ecol.

10 Model., 208, 91-101, 2007.

11 Muldavin, E. H., Moore, D. I., Collins, S. L., Wetherill, K. R., and Lightfoot, D. C.:

12 Aboveground net primary production dynamics in a northern Chihuahuan Desert ecosystem,

13 Oecologia, 155, 123-132, 2008.

14 Munkhtsetseg, E., Kimura, R., Wand, J., and Shinoda, M.: Pasture yield response to

15 precipitation and high temperature in Mongolia, J. Arid Environ., 70, 1552-1563, 2007.

16 Notaro, M., Liu, Z., Gallimore, R. G., Williams, J. W., Gutzler, D. S., and Collins, S.: Complex

17 seasonal cycle of ecohydrology in the Southwest United States, J. Geophys. Res., 115, G04034,

18 doi: 10.1029/2010JG001382, 2010.

19 Ogle, K., and Reynolds, J. F.: Plant responses to precipitation in desert ecosystems: integrating

20 functional types, pulses, thresholds and delays, Oecologia, 141, 282-294, 2004.

21 Okin, G. S., and Roberts, D.A.: Remote sensing in arid environments: challenges and

22 opportunities, in: Manual of Remote Sensing Vol 4: Remote Sensing for Natural Resource

23 Management and Environmental Monitoring, edited by: Ustin, S., John Willey and Sons, New

24 York, USA, 111-146, 2004.

25 Okin, G. S., Roberts, D. A., Murray, B., and Okin, W. J.: Practical limits on hyperspectral

26 vegetation discrimination in arid and semiarid environments, Remote Sens. Environ., 77, 212-

27 225, 2001.

28 Okin, G. S., Parsons, A. J., Wainwright, J., Herrick, J. E., Bestelmeyer, B. T., Peters, D. C., and

29 Fredrickson, E. L.: Do changes in connectivity explain desertification? BioScience, 59, 237-

30 244, 2009.

1 Pennington, D. D., and Collins, S. L.: Response of an aridland ecosystem to interannual climate

2 variability and prolonged drought, Landscape Ecology, 22, 897-910, 2007.

3 Peters, D. P. C.: Plant species dominance at a grassland-shrubland ecotone: and individual-

4 based gap dynamics model of herbaceous and woody species, Ecol. Model., 152, 5-32, 2002.

5 Peters, A. J., and Eve, M. D.: Satellite monitoring of desert plant community response to

6 moisture availability, Environ. Monit. Assess., 37, 273-287, 1995.

7 Peters, A. J., Eve, M. D., Holt, E. H., and Whitford, W. G.: Analysis of desert plant community

8 growth patterns with high temporal resolution satellite spectra, J. Appl. Ecol, 34, 418-432,

9 1997.

10 Petrie, M. D., Collins, S. L., Gutzler, D. S., and Moore, D. M.: Regional trends and local

11 variability in monsoon precipitation in the northern Chihuahuan desert, USA, J. Arid Environ,

12 103, 63-70, 2014.

13 Pockman, W. T., and Small, E. E.: The influence of spatial patterns of soil moisture on the

14 grass and shrub responses to a summer rainstorm in a Chihuahuan desert ecotone, Ecosystems,

15 13, 511-525, 2010.

16 Polley, H. W., Johnson, H. B., and Tischler, C. R.: Woody invasion of grasslands: evidence that

17 CO_2 enrichment indirectly promotes establishment of Prosopis glandulosa, Plant Ecol., 164,

18 85-94, 2002.

19 Prasad, V. K., Badarinath, K. V. S., and Eaturu, A.: Spatial patterns of vegetation phenology

20 metrics and related climatic controls of eight contrasting forest types in India-analysis from

21 remote sensing datasets, Theor Appl Climatol, 89, 95-107, 2007.

22 Ravi, S, Breshears, D. D., Huxman, T. E., and D'Odorico, P.: Land degradation in drylands:

23 Interactions among hydrologic-aeolian processes and vegetation dynamics, Geomorphology,

24 116, 236-245, 2010.

25 Reynolds, J. F., Virginia, R. A., Kemp, P. R., de Soyza, A. G., and Tremmel, D. C.: Impact of

26 drought on desert shrubs: effects of seasonality and degree of resource island development,

27 Ecol. Monogr., 69, 69-106, 1999.

28 Reynolds, J. F., Kemp, P. R., Ogle, K., and Fernandez, R. J.: Modifying the 'pulse-reserve'

29 paradigm for deserts of North America: precipitation pulses, soil water, and plant responses,

30 Oecologia, 141, 194-210, 2004.

1   Rietkerk, M., Boerlijst, M. C., Van Langevelde, F., HilleRisLambers, R., Van de Koppel, J.,
2   Kumar, L., Prins, H. H. T., and de Roos, A. M.: Self-organization of vegetation in arid
3   ecosystems, Am. Nat., 160, 524-530, 2002.

4   Roderick, M. L., Noble, I. R., and Cridland, S. W.: Estimating woody and herbaceous cover
5   from time series satellite observations, Global Ecol. Biogeogr., 8, 501-508, 1999.

6   Saco, P. M., and Moreno-de las Heras, M.: Ecogeomorphic coevolution of semiarid hillslopes:
7   emergence of banded and striped vegetation patterns through interaction of biotic and abiotic
8   processes, Water Resour. Res., 49, 115-126, 2013.

9   Schwinning, S. and Sala, O.E.: Hierarchy of responses to resource pulses in arid and semi-arid
10 ecosystems, Oecologia, 141, 211-220, 2004.

11 Schlesinger, W. H., Reynolds, J. F., Cunningham, G. L., Huenneke, L. F., Jarrell, W. M.,
12 Virginia, R. A., and Whitford, W. G.: Biological feedbacks in global desertification, Science,
13 247, 1043-1048, 1990.

14 Smith, M. O., Ustin, S. L., Adams, J. B., and Gillespie, A. R.: Vegetation in deserts: I. a
15 regional measure of abundance from multispectral images, Remote Sens. Environ., 31, 1-26,
16 1990.

17 Snyder, K. A., and Tartowsky, S. L.: Multi-scale temporal variation in water availability:
18 Implications for vegetation dynamics in arid and semi-arid ecosystems, J. Arid Environ, 65,
19 219-234, 2006.

20 Soil Survey Staff: Keys to Soil Taxonomy, 11th Ed., USDA Natural Resources Conservation
21 Service, Washington, USA, 2010.

22 Somers, B., Asner, G. P., Tits, L., and Coppin, P.: Endmember variability in Spectral Mixture
23 Analysis: A review, Remote Sens. Environ., 115,1603-1616, 2011.

24 Sparrow, A. D., Friedel, M. H., Stafford-Smith, D. M.: A landscape-scale model of shrub and
25 herbage dynamics in Central Australia, validated by satellite data, Ecol. Model., 97, 197-213,
26 1997.

27 Stewart, J., Parsons, A. J., Wainwright, J., Okin, G. S., Bestelmeyer, B. T., Fredrickson, E. L.,
28 and Schlesinger, W. H.: Modelling emergent patterns of dynamic desert ecosystems, Ecol.
29 Monogr., 84, 373-410, 2014.

1   Throop, H. L., Reichman, L. G., and Archer, S. R.: Response of dominant grass and shrub
2   species to water manipulation: an ecophysiological basis for shrub invasion in a Chihuahuan
3   Desert grassland, Oecologia, 169, 373-383, 2012.

4   Turnbull, L., Brazier, R. E., Wainwright, J., Dixon, L., and Bol, R.: Use of carbon isotope
5   analysis to understand semi-arid erosion dynamics and long-term semi-arid degradation, Rapid
6   Commun. Mass Sp., 22, 1697-1702, 2008.

7   Turnbull, L., Wainwright, J., and Brazier, R. E.: Changes in hydrology and erosion over a
8   transition from grassland to shrubland, Hydrol. Process., 24, 393-414, 2010a.

9   Turnbull, L., Wainwright, J., Brazier, R. E., and Bol, R.: Biotic and abiotic changes in
10 ecosystem structure over a shrub-encroachment gradient in the southwestern USA, Ecosystems,
11 13, 1239-1255, 2010b.

12 Turnbull, L., Wainwright, J. and Ravi, S.: Vegetation change in the southwestern USA: patterns
13 and processes, in: Patterns of Land Degradation in Drylands, Understanding Self-Organised
14 Ecogeomorphic Systems, edited by: Mueller, E. N., Wainwright, J., Parsons, A. J., and
15 Turnbull, L., Springer, New York, USA, 289-313, 2014.

16 Turnbull, L., Wilcox, B. P. , Belnap, J., Ravi, S., D'Odorico, P., Childers, D. L., Gwenzi, W.,
17 Okin, G. S., Wainwright, J., Caylor, K. K., and Sankey T.: Understanding the role of
18 ecohydrological feedbacks in ecosystem state change in drylands, Ecohydrology, 5, 174-183,
19 2012.

20 Turnbull, L., Parsons, A. J., Wainwright, J., and Anderson, J. P.: Runoff responses to long-term
21 rainfall variability in a shrub-dominated catchment, J. Arid Environ, 91, 88-94, 2013.

22 van Auken, O. W.: Shrub invasions of North American semiarid grasslands, Annu. Rev. Ecol.
23 Syst., 12, 352-356, 2000.

24 Veron, S. R., and Paruelo, V.: Desertification alters the response of vegetation to changes in
25 precipitation, J. App. Ecol., 47, 1233-1241, 2010.

26 Wainwright, J.: Climate and climatological variations in the Jornada Range and neighboring
27 areas of the US South West, Advances in Environmental Monitoring and Modelling, 1, 39-110,
28 2005.

1 Wainwright, J., Parsons, A. J., and Abrahams, A. D.: Plot-scale studies of vegetation, overland

2 flow and erosion interactions: case studies from Arizona and New Mexico, Hydrol. Process.,

3 14, 2921-2943, 2000.

4 Webb, R. H., Turner, R. M., Bowers, J. E., and Hastings, J. R.: The Changing Mile Revisited.

5 An Ecological Study of Vegetation Change with Time in the Lower Mile of an Arid and

6 Semiarid Region, University of Arizona, Tucson, USA, 2003.

7 Weiss, J. L., Gutzler, D. S., Coonrod, J. E. A., and Dahm, C. N.: Long-term vegetation

8 monitoring with NDVI in a diverse semi-arid setting, central New Mexico, USA, J. Arid

9 Environ., 58, 249-272, 2004.

10

1   **Table 1.** Main effects and interactions of seasonal precipitation (preceding non-monsoonal

2   rainfall, October-May; monsoonal summer rainfall, June-September; late non-monsoonal

3   rainfall, October-March) and landscape type (4 levels: grass-dominated, grass-transition,

4   shrub-transition, and shrub-dominated landscapes) on remote-sensing estimated annual (per

5   growing cycle, April-March) net primary production for herbaceous vegetation and shrubs.

	F	df	P	η^2 (%)
Herbaceous vegetation $ANPP_{r.sensing}$				
$Rain_{PNM\ (Oct-May)}$	194.2	1	0.000	4.2
$Rain_{SM\ (June-Sept.)}$	1483.4	1	0.000	**25.4**
$Rain_{LNM\ (Oct.-March)}$	129.3	1	0.000	2.0
LT	35.9	3	0.000	2.3
$LT:Rain_{PNM\ (Oct-May)}$	122.4	3	0.000	7.8
$LT:Rain_{SM\ (June-Sept.)}$	282.4	3	0.000	**16.2**
$LT:Rain_{LNM\ (Oct.-March)}$	1.1	3	0.326	0.0
Shrubs $ANPP_{r.sensing}$				
$Rain_{PNM\ (Oct-May)}$	1661.2	1	0.000	**27.7**
$Rain_{SM\ (June-Sept.)}$	1720.8	1	0.000	**28.4**
$Rain_{LNM\ (Oct.-March)}$	7.1	1	0.010	0.1
LT	2.9	3	0.030	0.2
$LT:Rain_{PNM\ (Oct-May)}$	6.6	3	0.000	0.4
$LT:Rain_{SM\ (June-Sept.)}$	46.2	3	0.000	3.0
$LT:Rain_{LNM\ (Oct.-March)}$	31.9	3	0.000	2.1

6   Abbreviations: $ANPP_{r.sensing}$, remote-sensed annual net primary production; $Rain_{PNM\ (Oct-May)}$,

7   preceding non-monsoonal rainfall; $Rain_{SM\ (June-Sept.)}$, monsoonal summer rainfall; $Rain_{LNM\ (Oct.-}$

8   $_{March)}$, late non-monsoonal rainfall; LT, landscape type; ':', interaction terms; η^2, eta-squared

9   (effect size).

10   Notes: η^2 values in bold are > 10% (effects that contribute in more than 10% to the total

11   variance comprised in $ANPP_{r.sensing}$).

12

1   **Fig. 1.** Simulated dryland biomass-rainfall relationships for herbaceous and shrub vegetation:

2   **(a)** modelled biomass dynamics for an herbaceous (green) and a shrub (red) species, **(b)**

3   strength of the biomass-precipitation relationship (Pearson's R correlation) using different

4   lengths of rainfall accumulation for the simulated herbaceous and shrub species (values above

5   the dotted grey line are significant at $P<0.05$), **(c)** optimal rainfall accumulation length (Olr)

6   as a function of the plant-growth and mortality rates. $ARain_{hv}$ and $ARain_s$ lines in panel (a)

7   represent the antecedent rainfall series that best correlate with the simulated series of

8   herbaceous and shrub biomass, respectively (i.e. time series of precedent rainfall with rainfall

9   accumulation lengths Olr_{hv} for herbaceous vegetation and Olr_s for shrubs). The green and red

10   dots in panel (c) indicate optimal rainfall accumulation lengths obtained for the simulated

11   herbaceous (Olr_{hv}, 52 days) and shrub (Olr_s, 104 days) species, respectively. The (grey)

12   "vegetation extinction" area in panel (c) reflects combined values of plant-growth and

13   mortality rates that do not support long-term vegetation dynamics for the simulated rainfall

14   conditions.

15

16   **Fig. 2.** Study area: **(a)** location of the Sevilleta National Wildlife Refuge (SNWR) and

17   distribution of major New Mexico biomes, **(b)** regional location of the study area (McKenzie

18   Flats, SNWR), **(c)** detailed location of the study site (18-km^2 area) and general view of the

19   reference SEV LTER Black Grama (right) and Creosotebush (left) Core Sites. Map (a)

20   follows the Sevilleta LTER classification of New Mexico biomes (Sevilleta LTER,

21   http://sev.lternet.edu/content/new-mexico-biomes-created-sevlter). Source for background

22   image in panels (b) and (c): 2009 National Aerial Imagery Program (USDA Farm Service

23   Agency).

24

25   **Fig. 3.** Reference NDVI-rainfall relationships at the SEV LTER Black Grama and

26   Creosotebush Core Sites: **(a)** 2000-13 MODIS NDVI time series for the Core Sites, **(b)**

27   strength of the NDVI-rainfall relationship (Pearson's R correlation) for the Core Sites using

28   different lengths of rainfall accumulation (maximum correlations, R_{max}, for the annual cycles

29   of vegetation growth are shown together with the 2000-13 mean trend; detailed correlograms

30   for each growing cycle can be found in Supplementary Fig. 1 as online supporting

31   information for this study). R values above the dotted grey line are significant at $P<0.05$.

32     $ARain_{hv}$ and $ARain_s$ lines in panel (a) represent the antecedent rainfall series that best correlate

1 with the NDVI series for the Black Grama and Creosotebush Core sites (i.e. time series of

2 precedent rainfall with rainfall accumulation lengths Olr_{hv} and Olr_s, respectively). Reference

3 Olr_{hv} and Olr_s values in panel (b) represent the optimal rainfall accumulation lengths for

4 herbaceous vegetation (57 days) and shrubs (145 days), respectively.

5

6 **Fig. 4.** Principal Component Analysis (PCA) of the NDVI-rainfall correlation coefficients for

7 the herbaceous- and shrub-specific antecedent rainfall series $ARain_{hv}$ and $ARain_s$ (57- and

8 145-day cumulative rainfall series, respectively) and resulting landscape type classification

9 across the 18 km^2 study area: **(a)** PCA projection of cases (MODIS pixels), **(b)** PCA

10 projection of variables (per growing cycle NDVI-antecedent rainfall correlation scores), **(c)**

11 landscape type classification (GD, grass-dominated, GT, grass-transition, ST, shrub-

12 transition, and SD, shrub-dominated landscapes) as a function of the relationship between

13 PCA Factor 1 and field-estimated vegetation dominance for a reference set of 27 control

14 points, **(d)** spatial distribution of landscape types in the study area, **(e)** general view and

15 characteristics of the landscape types. MODIS pixel locations for the ground control points

16 are highlighted in panel (a). Vector labels in panel (b) indicate the dates of the yearly cycles

17 of vegetation growth (April-March). Source for background image in panel (d): 2009 National

18 Aerial Imagery Program (USDA Farm Service Agency).

19

20 **Fig. 5.** NDVI decomposition and transformation into partial Annual Net Primary Production

21 (ANPP) components for herbaceous and shrub vegetation: **(a)** decomposed NDVI time series

22 of herbaceous and shrub vegetation for the reference SEV LTER Black Grama and

23 Creosotebush Core Sites, **(b)** relationships between field ANPP and the (per growing cycle)

24 annual integrals of herbaceous and shrub NDVI components for the SEV LTER Core Sites,

25 **(c)** remote-sensed ANPP estimates against field ANPP determinations (root mean square

26 error, RMSE, and normalized error, NRMSE, of the estimates are shown within the plot) **(d)**

27 remote-sensed ANPP estimations of herbaceous and shrub vegetation (mean for the 2000-13

28 series) , and **(e)** herbaceous and shrub contribution to total ANPP (mean for the 2000-13

29 series) across the 18-km^2 study area.

30

1   **Fig. 6.** Spatiotemporal dynamics of remote-sensed ANPP: **(a)** ANPP differences between

2   landscape types (grass-dominated, grass-transition, shrub-transition, and shrub-dominated

3   landscapes) along 2000-13, **(b)** 2000-13 temporal variations of the shrub contribution to total

4   ANPP for the different landscape types (Pearson's *R* correlations of shrub ANPP contributions

5   with time). Different letters in panel (a) for each cycle of vegetation growth indicate

6   significant differences between landscape types at $P<0.05$ (tested using repeated-measures

7   ANOVA and post-hoc Tukey HSD tests). Dotted lines in panel (b) represent weak ($R<0.40$)

8   correlations. Displayed correlations are significant at $P<0.05$. Numbers in plot (c) indicate

9   correlation coefficients.

10

11   **Fig. 7.** Scatter plots and correlations (Pearsons's *R*) between remote-sensed ANPP

12   estimations and seasonal precipitation (preceding non-monsoonal, summer monsoonal, and

13   late non-monsoonal rainfall) for the different landscape types (grass-dominated, grass-

14   transition, shrub-transition, and shrub-dominated landscapes): **(a)** herbaceous ANPP, **(b)**

15   shrub ANPP. Solid and dotted lines represent strong ($R\geq0.40$) and weak ($R<0.40$)

16   correlations, respectively. Displayed correlations are significant at $P<0.05$. Numbers within
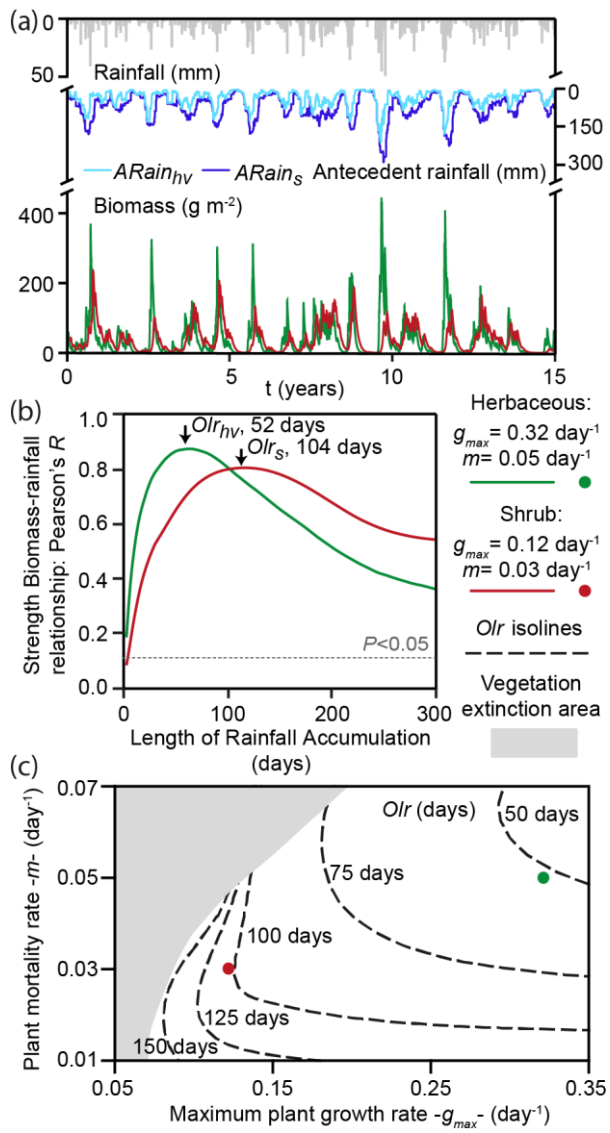
17   the plots indicate correlation coefficients.
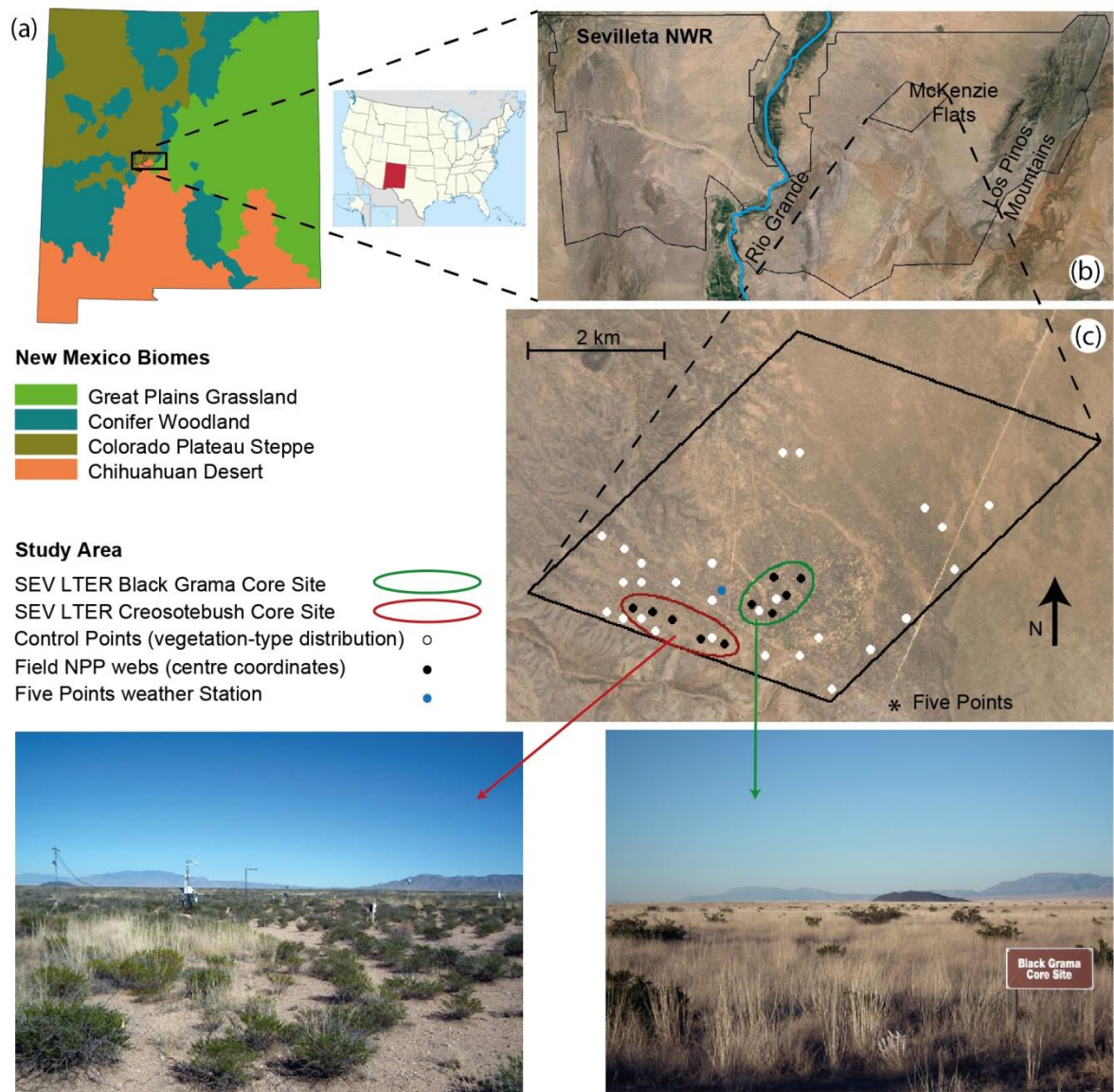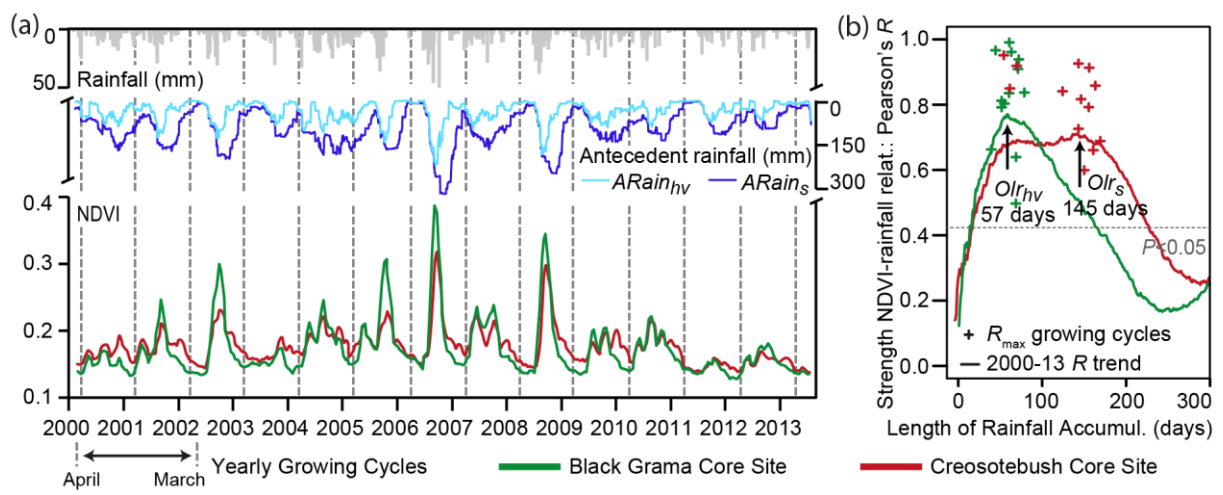
Fig. 1.

New Mexico Biomes

- Great Plains Grassland
- Conifer Woodland
- Colorado Plateau Steppe
- Chihuahuan Desert

Study Area

SEV LTER Black Grama Core Site
SEV LTER Creosotebush Core Site
Control Points (vegetation-type distribution)   ○
Field NPP webs (centre coordinates)   ●
Five Points weather Station   ●

Fig. 2.

Fig. 3.

(a) PCA projection of cases (MODIS pixels)

(b) PCA projection of variables (per cycle NDVI-rainfall correlation coefficients)

Contributors to Factor 1 (>5% variance)
Contributors to Factor 2 (>5% variance)
NDVI-$ARain_{hv}$ correlations
NDVI-$ARain_s$ correlations

(c) Dominance of vegetation forms and landscape type classification

- Shrubs
- Herbaceous vegetation

$y = 84.1 - 5.5x$
$R^2 = 0.87; P<0.001$

$y = 17.4 + 8.1x$
$R^2 = 0.89; P<0.001$

± SD

(e)

GD *Grass-dominated landscapes*
Dominance:
- Perennial grass > 65%
- Forbs > 20%
- Creosotebush < 30%

GT *Grass-transition landscapes*
Dominance:
- Perennial grass 65-50%
- Forbs 20-15%
- Creosotebush 30-50%

ST *Shrub-transition landscapes*
Dominance:
- Perennial grass 50-35%
- Forbs 20-15%
- Creosotebush 50-70%

SD *Shrub-dominated landscapes*
Dominance:
- Perennial grass < 35%
- Forbs < 15%
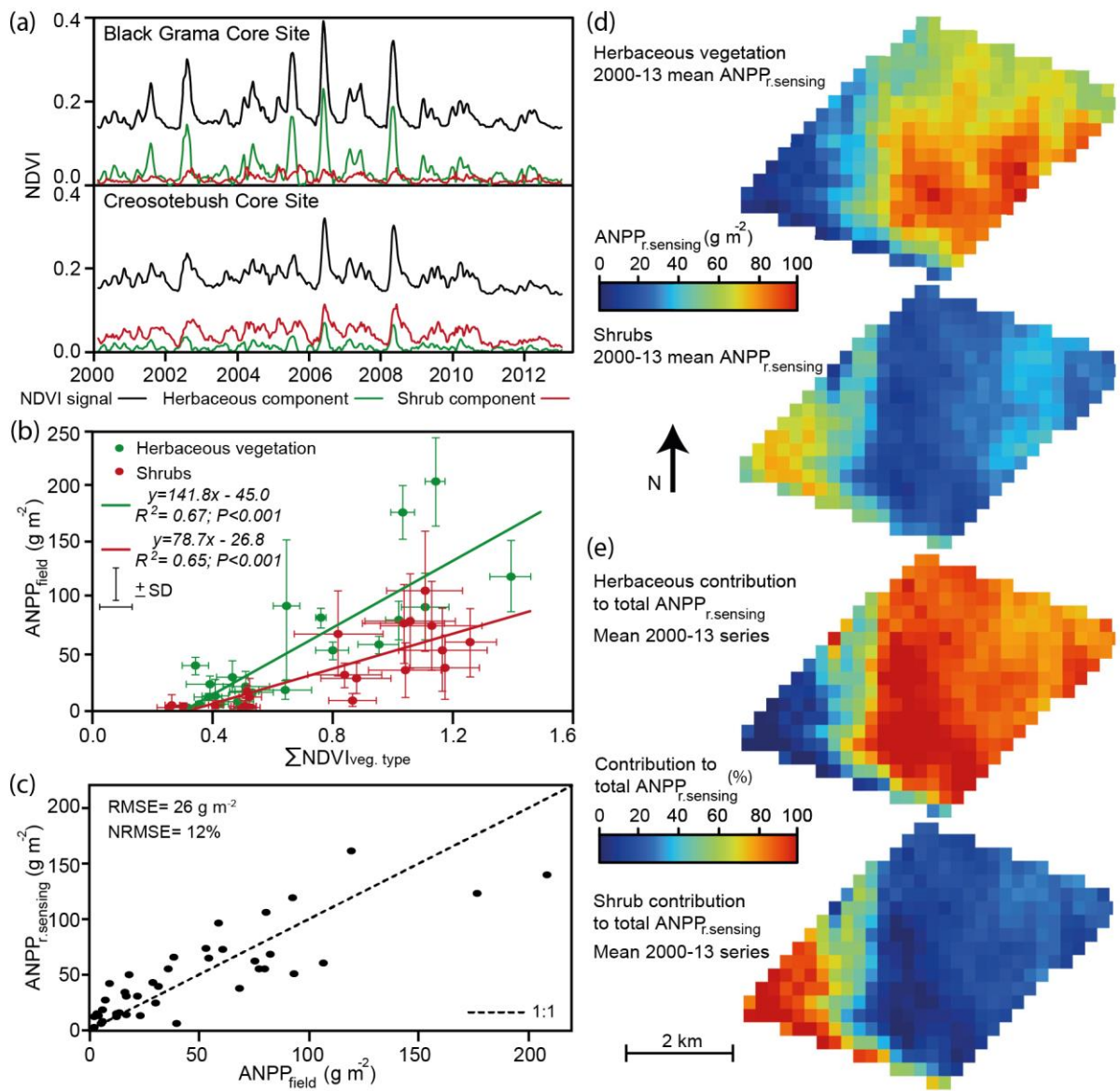- Creosotebush > 70%

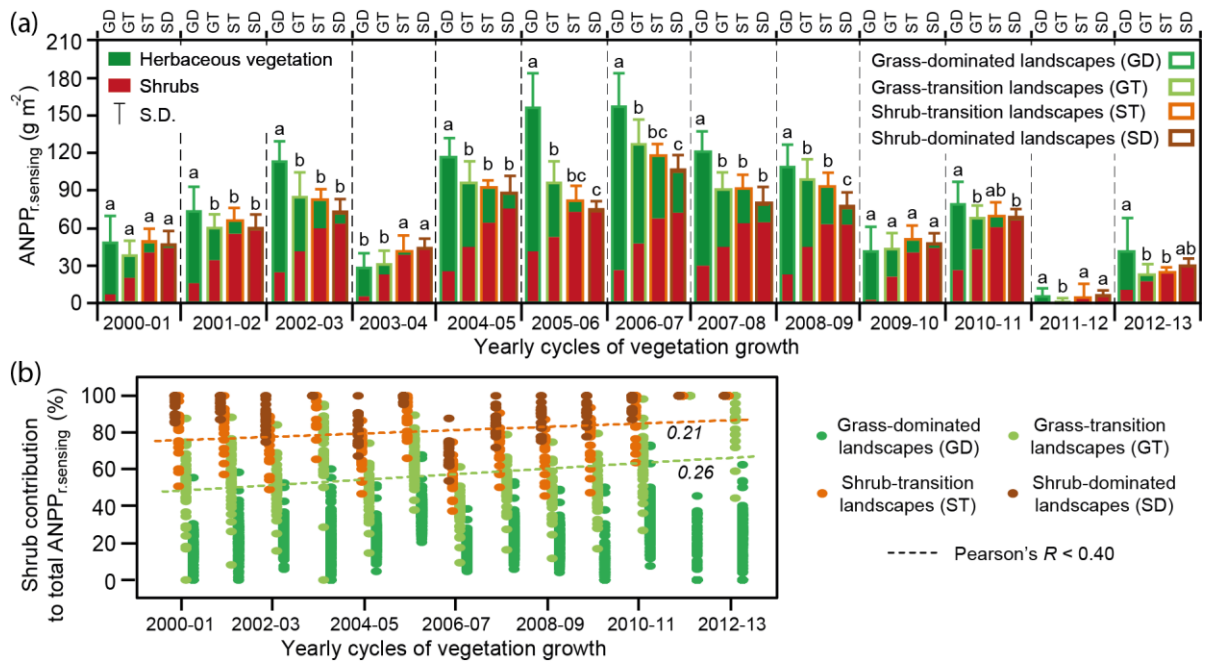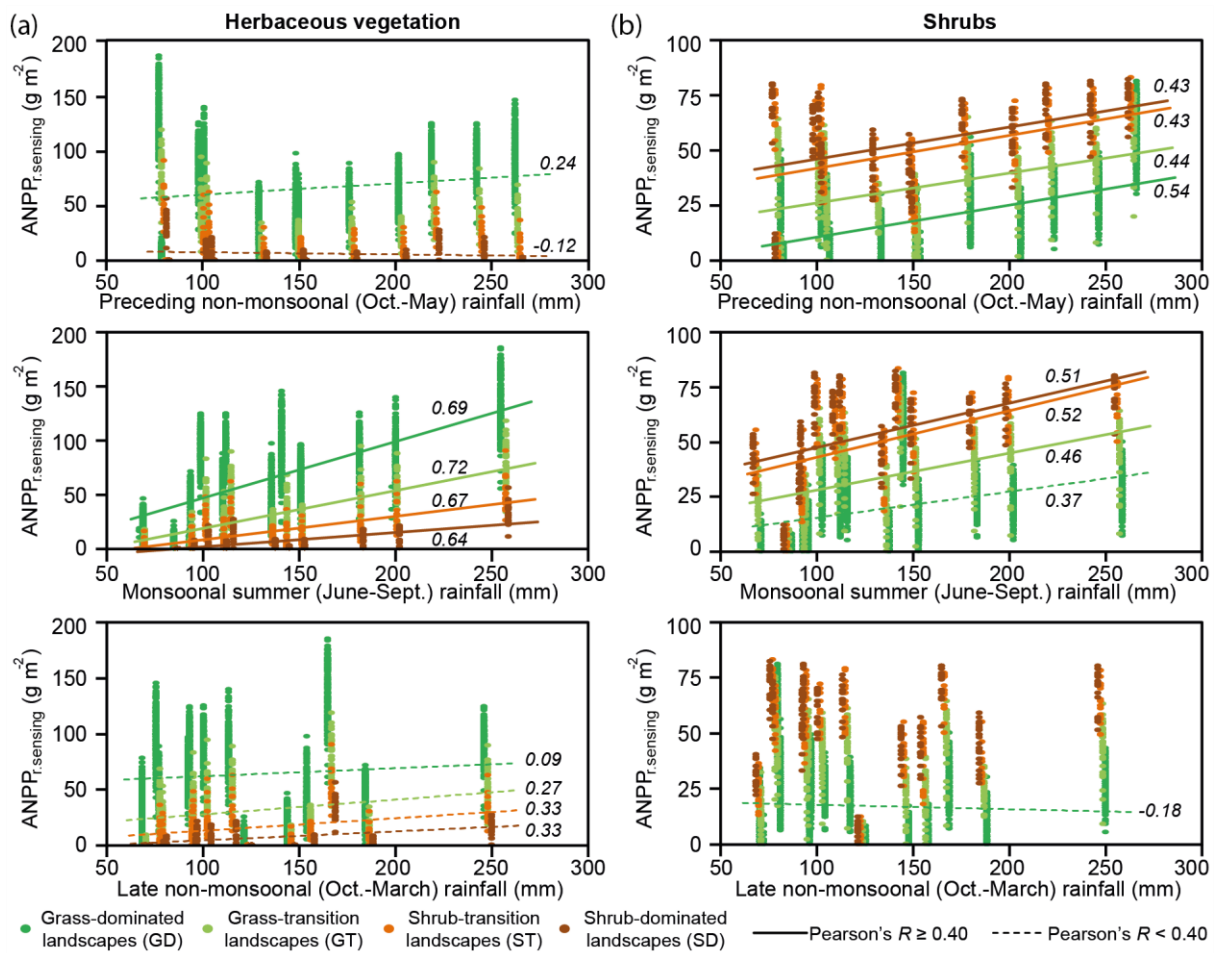**Fig. 4.**

40

Fig. 5.

Fig. 6.

1

Fig. 7.

1 In this document we provide the Maple 9.5 (Maplesoft, Waterloo, Canada) codes used in the

2 paper (Code 1) to simulate dryland biomass dynamics for an herbaceous and a shrub species,

3 and (Code 2) to decompose single time series of NDVI into partial components for

4 herbaceous and shrub vegetation applying the reference vegetation-type characteristic

5 antecedent rainfall series for herbs and shrubs ($ARain_{hv}$ and $ARain_s$, respectively). We also

6 provide two supplementary figures: (i) Supplementary Fig. 1 that presents the results of our

7 model sensitivity analysis, and (ii) Supplementary Fig. 2 that presents detailed NDVI-

8 antecedent rainfall correlograms obtained for each growing cycle of vegetation growth (April-

9 March) in the reference Black Grama and Creosotebush SEV LTER Core Sites.

10

11

12

13

14 Contents:

19

Code 1:   **Dynamic Vegetation Model**

Input files (location: C:\DataFolder\)**:**

1. Daily rainfall: Rain.txt

Data is stored in columns 1 and 2 for dates and rainfall, respectively.

Output files (location: C:\DataFolder\)**:**

1. Temporal series of herbaceous and shrub biomass: Biomass.txt

Data is stored in columns 1, 2 and 3 for dates, herbaceous and shrub biomass, respectively.

2. Temporal series of herbaceous and shrub biomass graph: Biomass.png (green, herbaceous

biomass; red, shrub biomass; blue, daily rainfall).

Procedure:

1. We load the Maple packages required for the subsequent calculations.

```
> with(linalg): with(plots): with(LinearAlgebra): with(Statistics): with(plottools):
```

2. We load the daily rainfall data file.

```
> droot := "C:\\DataFolder\\":
 drain := ImportMatrix(cat(droot, "Rain.txt"), source = delimited, delimiter = " ", datatype
= anything):
 dates := ImportMatrix(cat(droot, "Rain.txt"), source = delimited, delimiter = "",
datatype=string):
```

3. We define a rainfall function (rainFunct) made by rainfall event pulses.

```
> rainn := convert(Column(drain, 2), list):
 revent := [NULL]; raint := 0:
 for i to nops(rainn) do
 prec := convert(rainn[i], float):
```

```
1        if prec > 0 then

2        revent := [op(revent), [i, prec]]:

3        raint := raint+prec:

4        fi:

5        od:

6        rainFunct := t→sum(revent[jjk][2]*(-Heaviside(t-revent[jjk][1])+Heaviside(t-
7        revent[jjk][1]+1)), jjk = 1 .. nops(revent)):

8        ndata := nops(rainn);

9
```

10   *4. We define the model equations.*

```
11       > dB := gmax*(W-W0)*B/(W+kw)-m*B;

12       dW := P*(B+ki*i0)/(B+ki)-c*gmax*(W-W0)*B/(W+kw)-rw*W;

13       dsys := subs(W = W(t), B = B(t), [dB, dW]):

14       ecdif := [diff(B(t), t) = dsys[1], diff(W(t), t) = dsys[2]]:

15
```

16   *5. We define a time-evolution function (evolution) that calculates and stores biomass values*
17   *for each day, integrating the model equations with the model parameter values.*

```
18       > evolution := proc (param)

19        local stot, Biomasst, i:

20        stot := dsolve({op(subs(P = rainFunct(t), param, ecdif)), B(0) = 50, W(0) = .2}, numeric,
21       maxfun = 0):

22        Biomasst := NULL:

23        for i to ndata do

24        Biomasst := op([Biomasst]), subs(stot(i), B(t)):

25        od:

26        RETURN(Biomasst)
```

end proc:

6. *We define the parameter values and call the time-evolution function.*

```
> herbParam := W0 = 0.05, kw = 0.45, ki = 180, i0 = 0.2, c = 0.1, rw = 0.1, gmax = 0.32,
m = 0.05:
shrubParam := W0 = 0.05, kw = 0.45, ki = 180, i0 = 0.2, c = 0.1, rw = 0.1, gmax = 0.12, m
= 0.03:
herbBiomass := evolution({herbParam}):
shrubBiomass := evolution({shrubParam}):
```

7. *We plot the time series of herbaceous and shrub biomass along with precipitation.*

```
> topl := 700:
figherb := pointplot([seq([i, herbBiomass[i]], i = 1 .. nops([herbBiomass]))], connect =
true, color = green):
figshrub := pointplot([seq([i, shrubBiomass[i]], i = 1 .. nops([shrubBiomass]))], connect =
true, color = red):
figYears := [NULL]:
for iy to 16 do
figYears := [op(figYears), pointplot([[365*iy, 0], [365*iy, topl]], color = grey, connect =
true, linestyle = 3)]
od:
figPrecipt := NULL:
for i to ndata do if drain[i][2] > 0 then
figPrecipt := op([figPrecipt]), pointplot([[i, topl], [i, topl-4*drain[i][2]]], connect = true,
color = navy, thickness = 3):
fi:
od:
```

```
1    figures:= display(figherb, figshrub, figYears, figPrecipt):

2    display(figures);

3

4    8. We export the output files.

5    fout := cat(droot, "Biomass.txt"):

6    for i to ndata do

7    FileTools[Text][WriteLine](fout, cat(dates[i][1], " ", convert(herbBiomass[i], string), " ",
8    convert(shrubBiomass[i], string))):

9    od:

10   FileTools[Text][Close](fout):

11   plotsetup(png, plotoutput = cat(droot, "Biomass.png")):

12   display(figures);

13   plotsetup(default):

14
```

1 **Code 2:   NDVI Decomposition Procedure**

2

3 **Input files** (location: C:\DataFolder\)**:**

4 1. NDVI experimental data: case.txt

5 Data is stored in column 1.

6 2. Characteristic antecedent rainfall series for herbaceous and shrub vegetation ($ARain_{hv}$ and

7 $ARain_s$, respectively): totalAR.txt

8 Data is stored in columns 1 and 2 for herbaceous and shrub vegetation, respectively.

9 3. Time in days from the initial date: totalT.txt

10 Data is stored in column 1.

11

12 **Output files** (location: C:\DataFolder\)**:**

13 1. Temporal series of herbaceous and shrub NDVI components: HScomponents.txt

14 Data is stored in columns 1 and 2 for herbaceous and shrub biomass, respectively.

15 2. Graph with the temporal series of herbaceous and shrub NDVI, along with the original total

16 NDVI signal: HScomponents.png (black, original signal; green, herbaceous component; red,

17 shrub component).

18

19 **Procedure:**

20 *1. We load the Maple packages required for the subsequent calculations.*

21   > with(ExcelTools): with(plots): with(plottools): with(LinearAlgebra): with(Statistics):

22

23 *2. We define the NDVI bare soil component (0.12) and define a function, pair, to handle data*

24 *lists.*

25   nsoil := 0.12;

26   pair := proc (x, y)

27   [x, y]

28   end proc

1

2 *2. We load the data files and store data as lists. The following data lists are defined:*

3 *dataAR1 = antecedent rainfall series for herbaceous vegetation (57-day period, $ARain_{hv}$*

4 *series).*

5 *dataAR2 = antecedent rainfall series for shrubs (145-day period, $ARain_s$ series).*

6 *dataT = time (measured in days from the beginning of the series).*

7 *dataNDVI = original NDVI time series.*

8 *dataNDVI0 = NDVI data list without the soil base line.*

9 > droot := "C:\\ DataFolder \\":

10 dNDVI := ImportMatrix(cat(droot, "case.txt"), source = delimited, delimiter = "   ",

11 datatype = anything):

12 totalAR := ImportMatrix(cat(droot, "TotalAR.txt"), source = delimited, delimiter = "   ",

13 datatype = anything):

14 totalT := ImportMatrix(cat(droot, "totalT.txt"), source = delimited, delimiter = " "):

15 Ndata := op(rtable_dims(dNDVI)[1])[2]:

16 dataAR1 := [NULL]: dataAR2 := [NULL]: dataAR1N := [NULL]: dataAR2N := [NULL]:

17 dataT := [NULL]: dataNDVI := [NULL]: dataNDVI0 := [NULL]:

18 for i to Ndata do

19 dataAR1 := [op(dataAR1), evalf(totalAR[i][1])]; dataAR2 := [op(dataAR2),

20 evalf(totalAR[i][2])]; dataT := [op(dataT), evalf(totalT[i][1])]; dataNDVI :=

21 [op(dataNDVI), evalf(dNDVI[i][1])]; dataNDVI0 := [op(dataNDVI0), evalf(dNDVI[i][1]-

22 nsoil)]

23 od:

24

25 *4. We define a first-order least-squares optimization function (linearfit) that fits the partial*

26 *contribution of the herbaceous and shrub components to the time series of NDVI (filtered for*

27 *the base-line bare soil contribution, dataNDVI0) as a function of the vegetation-type specific*

1   *antecedent rainfall series that maximize the NDVI-precipitation relationships for herbaceous*

2   *vegetation (dataAR1, ARain$_{hv}$ series) and for shrubs (dataAR2, ARain$_s$ series).*

```
3   >linearfit := proc (TAR1, TAR2, Tiemp, NDVIst)
4   local AInput, DOutput, fitlinear, dparam, i, sumres;
5   global Total;
6   AInput := zip(pair, TAR1, TAR2); DOutput := NDVIst;
7   fitlinear := LinearFit([ar1, ar2], AInput, DOutput, [ar1, ar2], output = solutionmodule);
8   dparam := fitlinear:-Results("leastsquaresfunction"); sumres := fitlinear:-
9   Results("residualsumofsquares");
10  Total := [NULL]; for i to Ndata do Total := [op(Total), subs(ar1 = AInput[i][1], ar2 =
11  AInput[i][2], dparam+nsoil)] od:
12  RETURN(dparam, sumres):
13  end proc:
```

14

15 *5. We define a function that reassigns the predicted weights of the fitted vegetation*

16 *components (i.e. the percentage contribution of each vegetation type over the predicted totals*

17 *for any t$_i$) to match the original shape of the NDVI time series, obtaining the final NDVI*

18 *components for herbaceous vegetation and shrubs.*

```
19  > linDecomp := proc (TAR1, TAR2, NDVIst, fit)
20  local Ntotal, j, i, pre1, pre2, ratio;
21  global Nherb, Nshrub;
22  Nherb := [NULL]; Nshrub := [NULL]; Ntotal := [NULL];
23  for i to Ndata do
24  pre1 := subs(ar1 = TAR1[i], ar2 = 0, fit); pre2 := subs(ar1 = 0, ar2 = TAR2[i], fit);
25  if 0 <= pre1 and 0 <= pre2 then ratio := NDVIst[i]/subs(ar1 = TAR1[i], ar2 = TAR2[i], fit);
26  Ngrass := [op(Nherb), pre1*ratio]; Nshrub := [op(Nshrub), pre2*ratio] elif pre1 < 0 and 0
27  <= pre2 then Nherb := [op(Nherb), 0]; Nshrub := [op(Nshrub), NDVIst[i]] elif pre2 < 0
28  and 0 <= pre1 then Nherb := [op(Nherb), NDVIst[i]]; Nshrub := [op([Nshrub]), 0] else
29  print(errors); ratio := 1; Nherb := [op(Nherb), 0]; Nshrub := [op(Nshrub), 0] fi;
30  Ntotal := [op(Ntotal), Nherb[nops(Nherb)]+Nshrub[nops(Nshrub)]+nsoil] od;
31   RETURN(Nherb, Nshrub, Ntotal):
32  end proc:
```

6. We call the fitting and reassigning functions.

```
lfit1 := linearfit(dataAR1, dataAR2, dataT, dataNDVI0);
HerbShrubLineal := linDecomp(dataAR1, dataAR2, dataNDVI0, lfit1[1]):
```

7. We plot the time series of the NDVI signal (figOr), and the final NDVI components for herbaceous vegetation (figHerb) and shrubs (figShrub).

```
figOr := PLOT(CURVES(convert(sort(zip(pair, dataT, dataNDVI)), list))):
figHerb := PLOT(CURVES(sort(sort(zip(pair, dataT, Nherb)))), COLOR(RGB, 0, 1, 0)):
figShrub := PLOT(CURVES(sort(sort(zip(pair, dataT, Nshrub)))), COLOR(RGB, 1, 0, 0)):
display(figOr, figHerb, figShrub);
```

8. We export the output files.

```
fout := cat(droot, "HScomponents.txt"):
for i to Ndata do
FileTools[Text][WriteLine](fout, cat(convert(Nherb[i], string), " ", convert(Nshrub[i],
string))):
od:
FileTools[Text][Close](fout):
plotsetup(png, plotoutput = cat(droot, "HScomponents.png")):
display(figOr, figHerb, figShrub):
plotsetup(default):
```
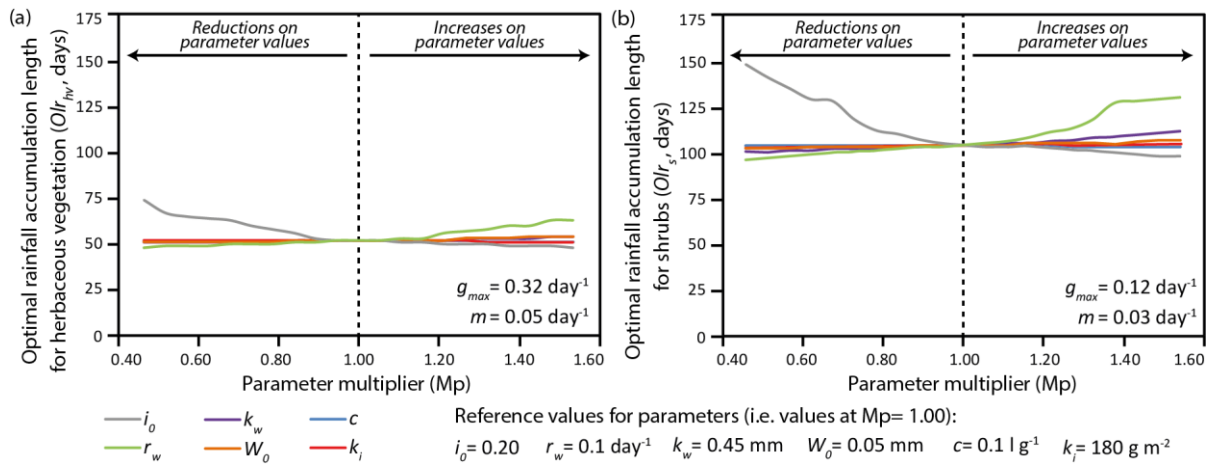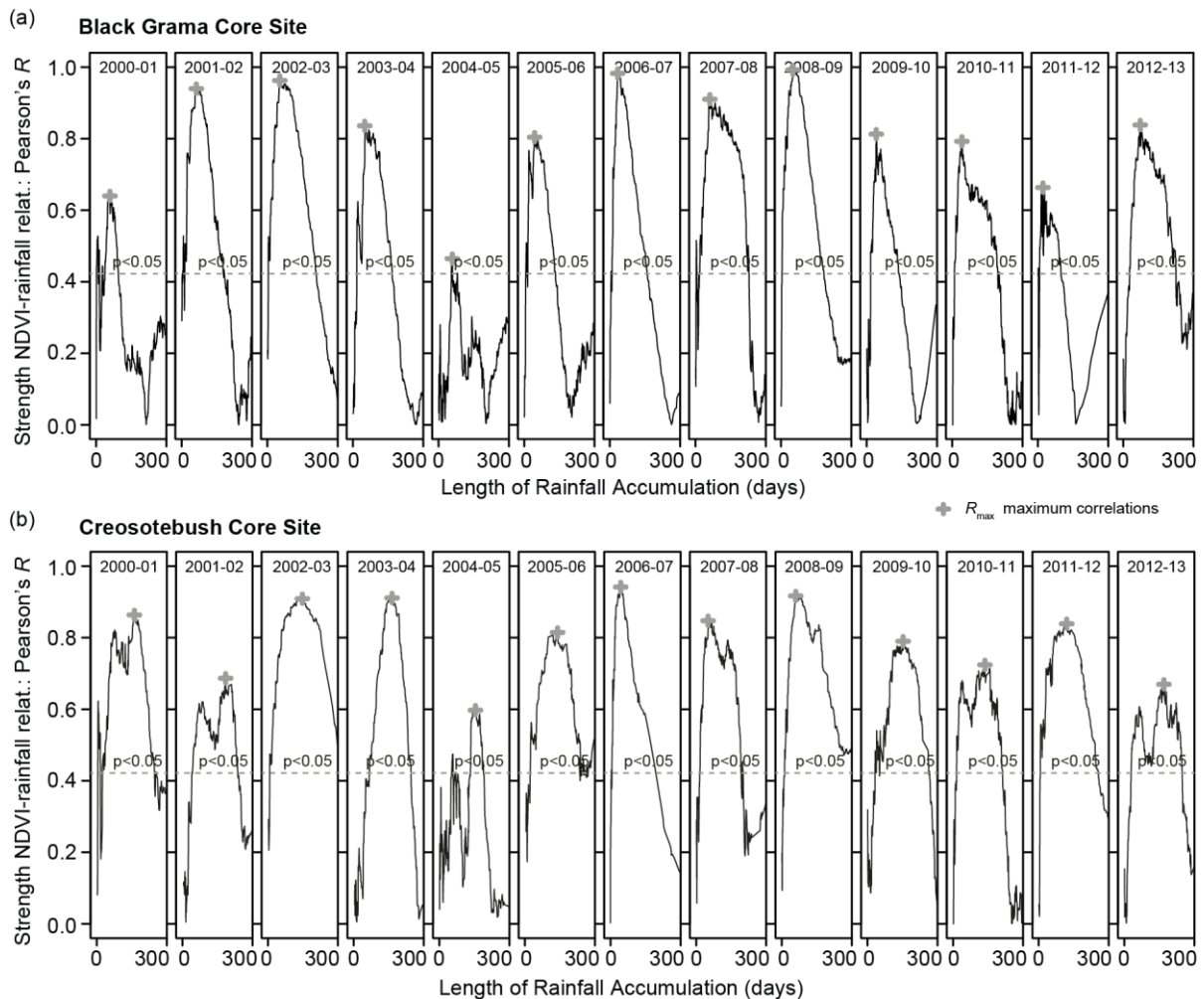
Supplementary Fig. 1. Sensitivity of simulated *Olr* values for herbaceous vegetation (**a**,

Olr$_{hv}$) and shrubs (**b**, *Olr$_s$*) to variations in model parameters i_0 (bare soil infiltration rate), r_w

(soil moisture evaporation/deep drainage rate), k_w (vegetation growth half saturation

constant), W_0 (permanent wilting point), c (plant-water-consumption coefficient), and k_i

(water infiltration half saturation constant). Parameter values applied in this study are shown

in the figure (i.e. reference values). Parameter variations to the reference values are

represented by the parameter multiplier (Mp), with Mp values <1 (and >1) showing

reductions (and increases) on parameter values. Maximum growth (g_{max}) and mortality (m)

rates applied in the study for herbaceous vegetation and shrubs are detailed within the plots.

Notes:

Variations on W_0, k_w, k_i, and c values have negligible effects on simulated *Olr*. Reductions on

bare soil infiltration (i_0) and increases on water loss by direct evaporation and/or deep

drainage (r_w) impact *Olr$_{hv}$* and *Olr$_s$* values, increasing time scale responses of vegetation to

antecedent precipitation, and ultimately amplifying the differences we obtained between

vegetation types.

1
2 **Supplementary Fig. 2.** Per annual growing cycle (April-March) NDVI-antecedent rainfall
3 correlograms for the **(a)** Black Grama and **(b)** Creosotebush SEV LTER Core Sites.
4 **Notes:**
5 Correlations between NDVI and antecedent precipitation are maximized using a rainfall
6 accumulation length of about 57 days for all annual cycles of vegetation growth in the Black
7 Grama Core Site (Supplementary Fig. 2a).
8 For the Creosotebush Core Site two different foci that maximize the correlation between
9 NDVI and antecedent rainfall can be detected: (i) one using a low rainfall accumulation
10 length (approx. 57 days) and (ii) another using a long rainfall accumulation length (approx.
11 145 days). The 145 days antecedent rainfall series generally shows a stronger correlation with
12 the NDVI than the 57 days antecedent rainfall series (cycles 2000-01, 2001-02, 2002-03,
13 2003-04, 2004-05, 2009-10, 2010-11, 2011-12, 2012-13). However, for three consecutive
14 annual cycles with strong summer precipitation (2006-07, 2007-08, and 2008-09, summer
15 precipitation for the period is 40% above the long-term mean) correlation of NDVI to the 57

1   days antecedent rainfall series is stronger than correlation to the 145 days antecedent rainfall

2   series (Supplementary Fig. 2b).